A review on experimental studies of surfactant adsorption at the hydrophilic solid–water interface

Santanu Paria*, Kartic C. Khilar

Department of Chemical Engineering, Indian Institute of Technology Bombay, Powai, Mumbai–400076, India

Abstract

The progresses of understanding of the surfactant adsorption at the hydrophilic solid–liquid interface from extensive experimental studies are reviewed here. In this respect the kinetic and equilibrium studies involves anionic, cationic, non-ionic and mixed surfactants at the solid surface from the solution. Kinetics and equilibrium adsorption of surfactants at the solid–liquid interface depend on the nature of surfactants and the nature of the solid surface. Studies have been reported on adsorption kinetics at the solid–liquid interface primarily on the adsorption of non-ionic surfactant on silica and limited studies on cationic surfactant on silica and anionic surfactant on cotton and cellulose. The typical isotherm of surfactants in general, can be subdivided into four regions. Four-regime isotherm was mainly observed for adsorption of ionic surfactant on oppositely charged solid surface and adsorption of non-ionic surfactant on silica surface. Region IV of the adsorption isotherm is commonly a plateau region above the CMC, it may also show a maximum above the CMC. Isotherms of four different regions are discussed in detail. Influences of different parameters such as molecular structure, temperature, salt concentration that are very important in surfactant adsorption are reviewed here. Atomic force microscopy study of different surfactants show the self-assembly and mechanism of adsorption at the solid–liquid interface. Adsorption behaviour and mechanism of different mixed surfactant systems such as anionic–cationic, anionic–non-ionic and cationic–non-ionic are reviewed. Mixture of surface-active materials can show synergistic interactions, which can be manifested as enhanced surface activity, spreading, foaming, detergency and many other phenomena.

Keywords: Surfactant adsorption; Adsorption kinetics; Adsorption isotherm; Solid–liquid interface; Mixed surfactant

Contents

* Corresponding author. *Present address*: Department of Chemical Engineering, Dalhousie University, 1360, Barington street, Halifax, Canada-B3J2X4. Tel.: +1-902-494-6212; fax: +1-902-420-7639.

E-mail addresses: sparia@iitb.ac.in, santanuparia@yahoo.com (S. Paria).

1. Introduction

Surfactant adsorption is a process of transfer of surfactant molecules from bulk solution phase to the surface/interface. The adsorption of surfactant at the solid–liquid interface play an important role in many technological and industrial applications, such as detergency, mineral flotation, corrosion inhibition, dispersion of solids, oil recovery and so on. One of the characteristic features of the surfactant is their tendency to adsorb at the surface/interface mostly in an oriented fashion. The phenomenon of surfactant adsorption has been studied to determine: (1) A measure of coverage of surface/interface by the surfactant, which in turn determines the performance of surfactant in many industrial processes. Such as foaming/defoaming detergency and emulsification. (2) The orientation of the surfactant molecules at the surface/interfaces, which in turn determines how the surface/interface will be affected by the adsorption, that is whether it will be become more hydrophilic or hydrophobic. These properties provide information on the type and the mechanism of any interactions involving the surfactant molecules at the surface/interface and its efficiency as a surface-active agent. The behaviour of surfactants at the interface is determined by number of forces, including electrostatic attraction, covalent bonding, hydrogen bonding, hydrophobic bonding and solvation of various species [1]. Here the review is mainly focused on the (1) surfactant adsorption kinetics on solid–liquid interface, (2) equilibrium adsorption studies of surfactant and (3) adsorption of mixed surfactant systems.

1.1. Hydrophilic solid surface chemistry

The hydrophilic solid is a characteristic of materials exhibiting an affinity to water. The surface chemistry allows these materials to be wetted forming a water film or coating on their surface. The surface functional groups have the ability to form the hydrogen bond with water. In general, mineral oxides and silica surfaces are used for studying surfactant adsorption at the hydrophilic surfaces. The solid–liquid interface is considered to develop a surface charge as a result of surface equilibrium involving potential determining ions which give rise to positive, negative and for some systems, neutral surface sites. The charge on the mineral colloids depends on the nature of the colloid, pH, ionic strength, and other solution conditions [2]. For oxides in simple electrolyte solution the charge is typically positive at low pH, the charge decreases and eventually becomes negative as pH increases. This charge variability is caused by the release and uptake of protons or hydroxyls. Generally, the H^+ and OH^- are the potential determining ions. Like other mineral oxide surfaces, the principal mechanism by which silica surfaces acquire a charge in contact with water and potential determining ions (H^+ and OH^-) is shown by the following equations [3]:

$$\mathrm{SiOH} + \mathrm{H^+} = \mathrm{SiOH_2^+}, \tag{1}$$

$$\mathrm{SiOH} + \mathrm{OH^-} = \mathrm{SiO^-} + \mathrm{H_2O}. \tag{2}$$

The isoelectric point of silica occurs at approximately pH 2 and the charge becomes negative between pH 6 and 11.

1.2. Mechanisms of surfactant adsorption

There are number mechanisms by which surface-active molecules may adsorb onto the solid substrates from aqueous solution [4]. In general, the adsorption of surfactants involves single ions rather than micelles [5].

i. *Ion exchange*: Replacement of counter ions adsorbed onto the substrate from the solution by similarly charged surfactant ions.
ii. *Ion pairing*: Adsorption of surfactant ions from solution onto oppositely charged sites unoccupied by counter ions.
iii. *Hydrophobic bonding*: Adsorption occurs by this mechanism when there is an attraction between a hydrophobic group of adsorbed molecule and a molecule present in the solution.
iv. *Adsorption by polarization of π electrons*: When the surfactant contains electron-rich aromatic nuclei; the solid adsorbent has strongly positive sites, attraction between electron rich aromatic nuclei of the adsorbate and positive sites on the adsorbent results in adsorption.
v. *Adsorption by dispersion forces*: Adsorption by London–van der Waals force between adsorbate and adsorbent increases with the increasing molecular weight of the adsorbate.

1.3. Practical applications

1.3.1. Mineral/particulate flotation

Ore or mineral flotation is currently the most industrially important example of a particulate flotation process and may be considered as a model for the other particulate process. Particulates, which have been successfully removed from suspension by flotation, include bacterial spores, algae, clays and colloidal precipitates [6]. Like ore flotation, each of these processes requires the addition of a suitably charged surfactant and either adjustment of pH or addition of an ion that promotes the adsorption of surfactant on the surface of the particulate.

1.3.2. Surfactant-enhanced carbon regeneration

Adsorption beds containing activated carbon are widely used to remove organic pollutants from wastewater streams. The adsorber will not be effective when breakthrough occurs and the carbon must be regenerated, this involves the removal of adsorbed organics from the carbon surface. In this method, a concentrated surfactant solution is passed through the adsorber containing the spent carbon, and the adsorbate desorbs and gets solubilised in the micelles [6].

1.3.3. Herbicide dispersions

In the present-day, the success of weed control technology in agriculture is attributable to the development and effective use of organic herbicides, followed by the use of herbicide adjuvants, particularly, the surfactants. Surfactants perform a number of different functions in herbicide dispersions. Surfactants are primarily used in aqueous dispersions, where they reduce the surface tension and consequently increase the spreading and wetting of the weed surface. This results in a uniform coverage of weed surface, greater absorption, reduced rate of evaporation, and other desirable effects [7]. Surfactants help herbicide molecules to penetrate through the waxy surface of leaf. In nitrogen containing fertilizer (ammonium sulfate)-surfactant blends help the nitrogen compound to penetrate through the leaf surface. Generally, mixture of non-ionic surfactants is used in these applications.

1.3.4. Deinking from paper and plastic film

Flotation deinking is the most important method for recycling of the paper. In this process, the surfactants are necessary for the removal of ink from the fibre during pulping step and to cause the pigment particles to be separated from the paper fibres by flotation. It is also important for the plastic recycling. The cationic surfactants are the most effective while the anionic surfactants are the least effective in removing the printing ink from plastic film, probably because the binder is an acidic acrylate with a negative charge [8].

1.3.5. Filtration of ultra fine particles

The removal of particulate contaminants is very important in many industries, such as water reclamation facilities, water treatment, microelectronics and pharmaceutical industries. As the size of the particles decreases particle removal becomes very difficult. Adsorption of proper surfactant on the filter surface can lower the energy barrier between the particles and the filter surface; and thus increase the deposition of small particles on the surface of the filter. One example of such phenomenon is micro porous polypropylene membrane filters which are modified with a cationic surfactant, dimethyldioctadecylammonium bromide (DDAB), to create a charged surface. Negatively charged nanoparticles can then be filtered by utilizing the electrostatic interaction between the charged particles and the polar head of the surfactants adsorbed on the filters [9].

1.3.6. Stability of particulate suspension

The stability of particle and colloidal slurries is an important phenomenon in many industries such as paint, printing ink, pharmaceutical, etc. Particle settling, which destabilizes the suspension, is often caused by the shielding of surface charges on the particles which would result in coagulation and subsequent settling. It has been found that the effects of addition of conventional stabilizing agents (e.g. ionic surfactants, polymers) increase the stability of the particle. However, sometimes the synergistic effects of

mixed ionic–non-ionic surfactant systems are used to improve the stability of particle suspension [10,11], especially when the system has high ionic strength [12].

1.3.7. Detergency

Surfactants molecules are adsorbed on both soil and fabric surface in the process of detergency. The adsorption of surfactants play a dual role in the removal of soil. They reduce the attraction between soil and fabric by attaching themselves to both. This way they not only loosen the soil from the fabric but also deflocculate the particles at the same time, i.e. they break up into colloidal particles and stabilize their aqueous dispersion. The soil, which forms a fine and stable dispersion in the wash liquor, is much less prone to attach itself to the fabric during remaining wash cycle than the soil present as a coarse and unstable dispersion. The detergency of a surfactant in the absence of electrolyte can be enhanced if the surfactant adsorption is enhanced [13].

2. Surfactant adsorption kinetics

Reported studies on the surfactant adsorption kinetics on the solid–liquid interface are limited when compared to that on the fluid–fluid interface. Studies of surfactant adsorption or desorption kinetics from water at the hydrophilic solid surface, have been conducted mostly by using silicon oxide (silica) [14–20], as this model hydrophilic surface has been well characterized. Adsorption kinetics on cotton [21,22], on filter paper [23] and on active carbon [24] have also been studied. There seems to be consequences in the literature to the time variations on extent of adsorption can be divided into three different regimes, they are: (1) linear increase in adsorption with time, (2) transition regime where the rate of adsorption levels off and (3) a plateau regime. The range over which the regions extend varies with the bulk concentration, nature of surfactant, presence of salt and so on. The nature of solid surface, that is the hydrophobic or hydrophilic, and the electrical interactions play an important role in the kinetics of adsorption of surfactant at the solid–liquid interface.

2.1. Adsorption kinetics of ionic surfactant

Biswas and Chattoraj [20] have studied the adsorption of cationic surfactants (C_{16}TAB, C_{14}TAB, C_{12}TAB) on silica–water interface at different bulk concentration, pH, ionic strength, temperature and electrolyte. It is shown that the adsorption follows a two-step first order rate process with two different process rate constants. We have studied the adsorption kinetics of anionic, cationic and non-ionic surfactant at the cellulose–water interface are shown in Fig. 1. It is shown that the rate of adsorption kinetics of cationic surfactant is very fast and the final amount adsorbed is higher than the anionic and non-ionic surfactant at the cellulose–water interface. The order of rate of adsorption

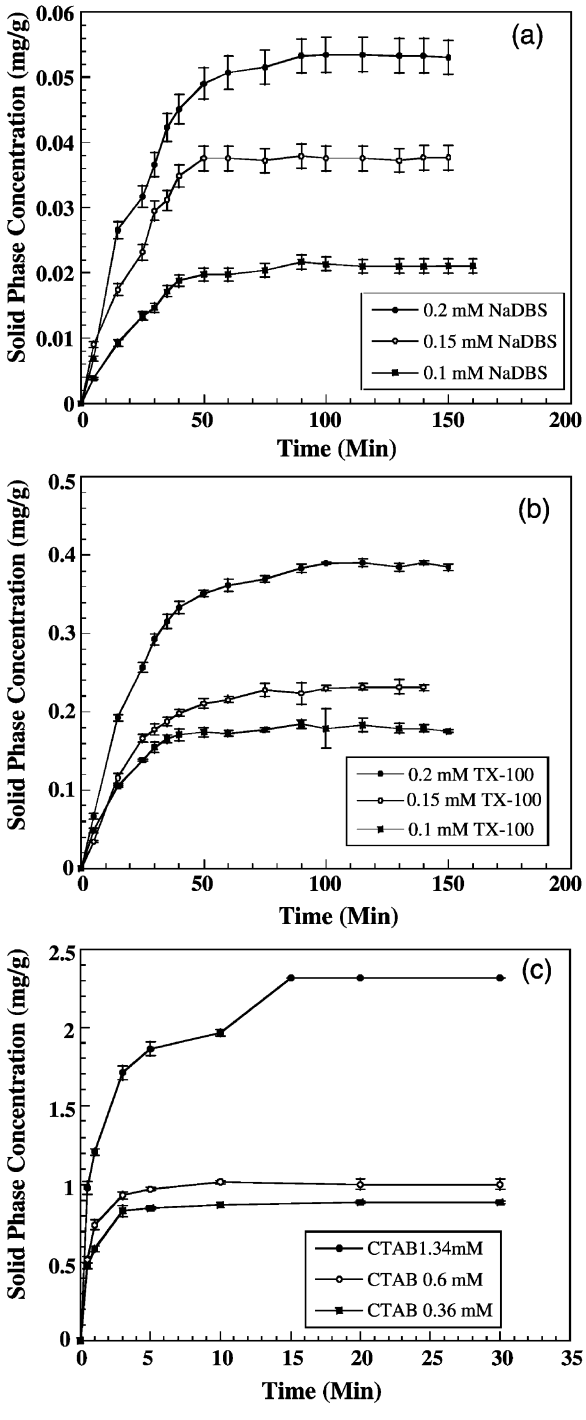

Fig. 1. (a) Adsorption kinetics of NaDBS. (b) Adsorption kinetics of TX-100. (c) Adsorption kinetics of CTAB on filter paper [23].

is cationic > anionic ≈ non-ionic. The average rate of adsorption of cationic, anionic and non-ionic was determined from the slope of at $t_{1/2}$ (half equilibrium time) of the adsorption curve. As the cellulose surface is negatively charged in the aqueous medium, so the cationic surfactant can preferably be adsorbed on the cellulose surface. Adsorption kinetics of anionic surfactant on cotton [21,22] shows that the total equilibrium time is approximately 2–3

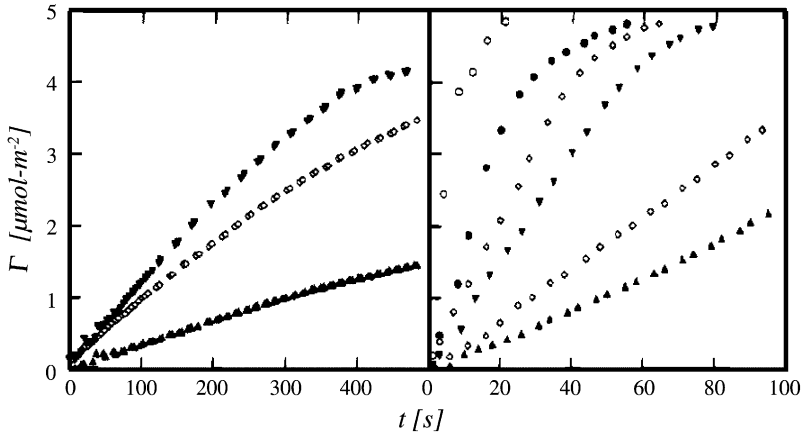

Fig. 2. Evolution of the adsorbed amount, Γ, of $C_{14}E_6$ with time at different surfactant concentrations ≤cmc, left side, and concentrations >cmc, right side. The initial adsorption rate increases steadily with the surfactant concentration, which is 0.007, 0.009, and 0.01 mmol l^{-1}, respectively, in the graph on the left side. The corresponding values in the plot on the right side are 0.02, 0.025, 0.05, 0.1, 0.25, and 1 mmol l^{-1}, respectively. Reproduced with permission from Ref. [17].

h and at least 50% adsorption was complete within 10 min and the rate of adsorption of anionic surfactant on cotton increases with the increasing temperature [21]. Biawas and Chattoraj [20] have also observed the rate constant of adsorption of CTAB, MTAB and DTAB on silica increases with increasing temperature.

2.2. Adsorption kinetics of non-ionic surfactant

Adsorption kinetics of non-ionic surfactant on silica has been studied by ellipsometry technique [14–17] and by UV absorption [19]. Fig. 2 shows the adsorption kinetics of $C_{14}E_6$ on silica–water interface. The initial adsorption rate increases with the increasing surfactant concentration. Kinetics model of adsorption of non-ionic surfactant on hydrophilic silica have been developed [14–16], considering the three processes that occurs in the solution: monomer diffusion, micellar diffusion and micellar dissociation. It is assumed that micelles do not adsorb on the hydrophobic surface. Fig. 3 represents a schematic picture of the process out side the silica surface. The adsorption was described as a two-step process, where the first step was diffusion from the bulk solution to a subsurface, and second step was transportation from the subsurface to the surface and the concomitant adsorption. The stagnant layer outside the surface was assumed to be finite due to the convection caused by stirring during measurements. The adsorption was observed to be diffusion controlled, and the concentration immediately outside the surface was determined by a local equilibrium in the sub-layer region. The micelles were assumed to contribute to the adsorption only by releasing monomers during the diffusive transport and not by direct adsorption. The initial increase in adsorption is approximately linear with time. The rate of adsorption in the linear region for the pre-micellar solutions, shows the linear function of bulk concentration, the csac (critical surface aggregation concentration), the thickness of the stagnant layer and diffusion coefficient of the monomer. Similar relation was found for the concentration above the CMC. As the amount adsorbed approaches the plateau value, the adsorption rate begins to decrease and finally becomes zero. Brinck et al. [15] have extended this model to the mixed surfactant system to

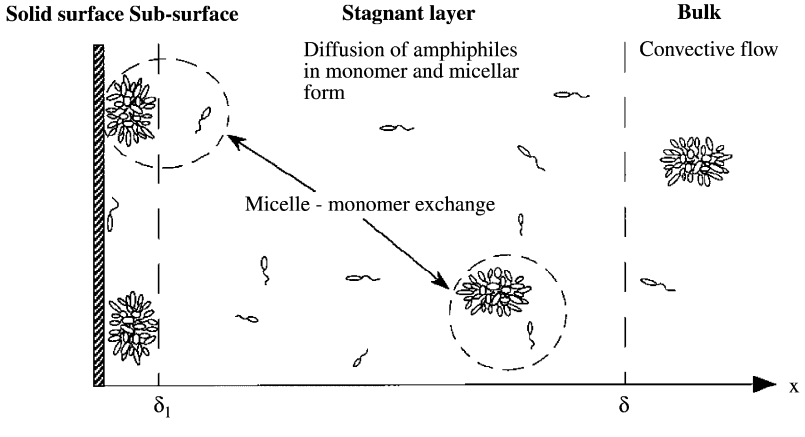

Fig. 3. Schematic presentation of the solution profile outside the silica surface. Reproduced with permission from Ref. [14].

predict the kinetic behaviour of binary mixture of non-ionic surfactants at silica–water interface.

3. Equilibrium adsorption of surfactant (adsorption isotherm)

The study of equilibrium of surfactant adsorption is important to determine the maximum amount adsorbed per unit area or mass of the adsorbent and to determine the adsorption isotherm. At the solid–liquid interface, the plot of amount of surfactant adsorbed per unit mass or unit area of the solid by varying the concentration of the adsorbate vs. equilibrium concentration is called adsorption isotherm. This is a measure of extent of surface of the adsorbent that is covered by the adsorbent molecules at a given condition, and hence determines the interfacial properties in many applications. Most of the interfacial processes are related to the equilibrium adsorption of the surfactant.

3.1. Adsorption of ionic surfactant

A number of studies have been conducted on the adsorption of anionic [21–45] and cationic [18,24,29,40,46–62] on the solid–liquid interface. The solid surfaces are either positively or negatively charged in the aqueous medium by ionisation/dissociation of surface groups or by the adsorption of ions from solution onto a previously uncharged surface. Therefore, the electrical double layer at the solid–liquid interface is usually an important phenomenon for the adsorption of ionic surfactants.

3.1.1. Surface charge and electrical double layer

At any interface, there is always an unequal distribution of electrical charges between the two phases. This unequal distribution causes one side of the interface to acquire a net charge of a particular sign and the other side to acquire a net charge of opposite sign, giving rise to a potential across the interface and so-called 'electrical double layer'. Since the overall electrical neutrality must be maintained, the net charge on one side of the interface must be balanced by an exactly equal net charge of opposite sign on the other side of the interface. Fig. 4 shows the schematic presentation of electrical double layer. The mathematical analysis of electrical double layer gives the term κ, the length scale for the screening and $1/\kappa$ is associated with the thickness of the ionic atmosphere around each ion and is called as the Debye length [63]. This is the distance from the charged surface into the solution within which the major portion of the electrical interactions with the surface can be considered to occur. The Debye length is given by the expression [63]:

$$\frac{1}{\kappa} = \left(\frac{\varepsilon\varepsilon_0 k_B T}{e^2 \sum C_i z_i}\right)^{\frac{1}{2}}, \tag{3}$$

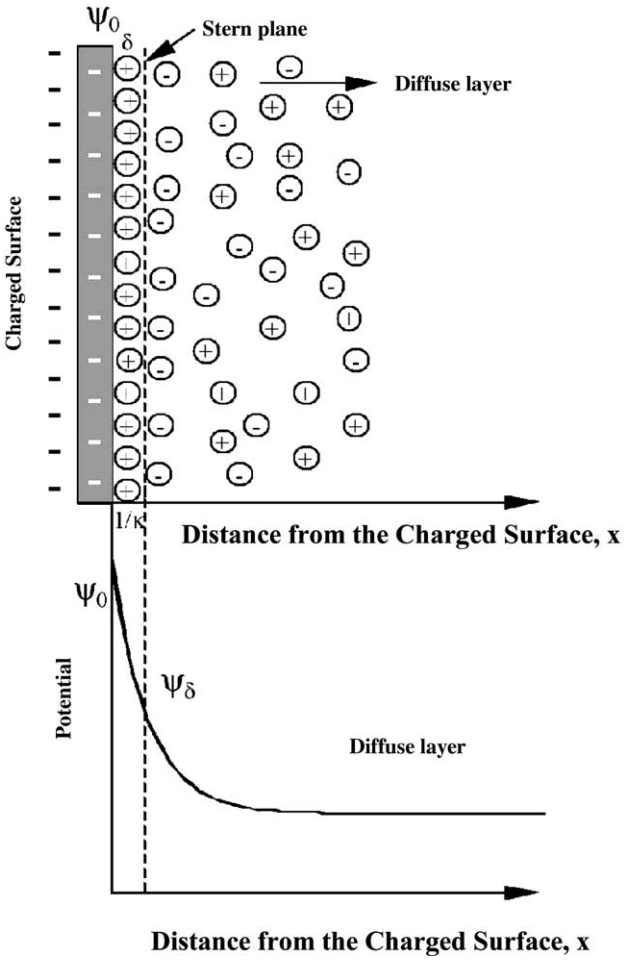

Fig. 4. Schematic presentation of electrical double layer.

where ε, ε_0 are the dielectric constants or permittivity of the solution and in vacuum, respectively, (J^{-1} m^{-1}), k_B, T, e, C, z are the Boltzmann constant, absolute temperature, charge of electron, molar concentration of ion in solution and valency of ion in solution, respectively. From the relationship, it is noted that $1/\kappa$ is inversely proportional to valance z of the ions and to the square root of their concentrations. It is also noted that the solvent with high dielectric constant such as water show higher electrical effect than the solvent with low dielectric constant. In addition, it can be shown that in the presence of electrolyte, electrical effects have shorter ranges or the electrical double layer is compressed.

3.1.2. Contributions to adsorption energy

Much attention has been given to understand the various contributory mechanisms to the adsorption process for wide variety of surfactants and adsorbents. The free energy of adsorption ΔG^0_{ads}, which is the sum of number of additive contributions, can be written as [64]:

$$\Delta G^0_{ads} = \Delta G^0_{elec} + \Delta G^0_{spec}, \tag{4}$$

where ΔG^0_{elec} accounts for the electrical interactions and ΔG^0_{spec} is a specific adsorption term, which contains all other contributions to the adsorption free energy that are dependent on the 'specific' (non-electrical) nature of the system. Using Stern–Grahame equation ΔG^0_{ads} can be calculated as to [1]:

$$\Gamma = rC_{eq}\exp\left(\frac{-\Delta G^0_{ads}}{RT}\right), \quad (5)$$

where r is the radius of the adsorbed ion and C_{eq} is the equilibrium concentration.

3.1.3. Electrical interactions

Usually, ΔG^0_{elec} is ascribed totally to the columbic interactions. However, the dipole term can be included in the electrical term such that [25]:

$$\Delta G^0_{elec} = \Delta G^0_{coul} + \Delta G^0_{dip}, \quad (6)$$

$$\Delta G^0_{coul} = zF\psi_\delta, \quad (7)$$

$$\Delta G^0_{dip} = \sum_j \Delta n_j \mu_j E_{ads}, \quad (8)$$

where ΔG^0_{coul} and ΔG^0_{dip} is the free energy term for columbic dipole, respectively, ψ_δ is the potential at the stern plane (δ is the thickness of the compact part of the double layer), Δn_j is the number of adsorbed molecules j, μ_j is the dipole moment of j and E_{ads} is electric field strength across the plane of adsorbed species.

If we neglect ΔG^0_{dip}, the basic interpretation of ΔG^0_{elec} will be simplified and there will be three cases [64];

i. When the surfactant ions are counter ions, then z and ψ_δ are of opposite sign, so, $zF\psi_\delta < 0$ and the electrical interaction promotes the adsorption process. This situation will exist for a cationic surfactant/negatively charged surface and anionic surfactant/positively charged surface.
ii. If the net charge density ($\sigma_0 + \sigma_\delta$) is of same sign as the surfactant ions, then z and ψ_δ are of same sign and $zF\psi_\delta > 0$, i.e. the electrical interaction opposes adsorption. In the absence of specifically adsorbed ions, this situation will exist for anionic surfactant/negatively charged surface and cationic surfactant/positively charged surface.
iii. Under i.e.p. (isoelectric point) conditions referred to above, ΔG^0_{elec} will be zero (neglecting ΔG^0_{dip}) and adsorption is governed by ΔG^0_{spec} term.

3.1.4. Specific interactions

ΔG^0_{spec} can be subdivided into separate independent interactions. The contributing force can be written as [1]:

$$\Delta G^0_{spec} = \Delta G^0_{chem} + \Delta G^0_{c-c} + \Delta G^0_{c-s} + \Delta G^0_{H} + \Delta G^0_{H_2O} \ldots, \quad (9)$$

ΔG^0_{chem} is the chemical term due to covalent bonding. ΔG^0_{c-c} is the lateral interaction term owing to the cohesive chain–chain interaction among adsorbed long chain surfactant species, usually important for Hemimicellization. ΔG^0_{c-s} is a similar interaction between the hydrocarbon chains and hydrophobic sites on the solid, ΔG^0_{H} is the hydrogen bonding term and $\Delta G^0_{H_2O}$ is the solvation or desolvation term, owing to the hydration of the adsorbate species or any species displaced from the interface due to adsorption.

3.1.5. Four-region adsorption isotherm

Fig. 5 presents the typical isotherm of adsorption of surfactants on the solid–liquid interface in a rather wide range of concentration of surfactants going beyond the CMC. In general, a typical isotherm can be subdivided into four regions when plotted on a log–log scale [13,33,35,39,40,44,45,53,60,61,65–68]. In region I, the adsorption obeys Henry's law, adsorption increases linearly with concentration and the slope of the curve is approximately one [41]. Region I, occurs at low concentration of surfactant and monomers are electrostatically adsorbed to the substrate [59]. Region II shows a sudden increase in the adsorption due to lateral interaction between the adsorbed monomer, resulting surface aggregation of the surfactants. Region III shows a slower rate of adsorption than region II. Region IV is the plateau region above the CMC [33,35,39,40,45,60,61,65–67]. However, depending upon several factors the region IV may show a maximum [18,21,22,26–29,32,44,46–49]. The systems that have shown this four region adsorption isotherms are shown in Table 1. In Table 1, the four-regime adsorption isotherm mainly occurs by adsorption of ionic surfactant onto oppositely charged solid surface.

The explanations for the nature of adsorption curve in the first three regimes are well accepted. The sudden rise in adsorption in region II is due to formation of surface

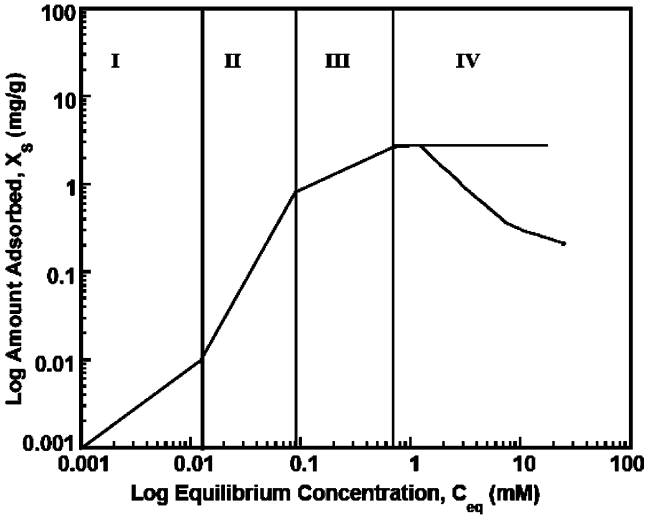

Fig. 5. Schematic presentation of typical four-regime adsorption isotherm. [44].

Table 1
Four-regime adsorption isotherm of different surfactants and solid–liquid systems

Surfactant	Adsorbent
Sodium dodecyl sulfonate	Alumina [35]
Alkyl benzene sulfonate	Alumina [33]
Tetradecyl Pyridium chloride (TPC)	Silica gel [53]
Tetradecyl Pyridium bromide (TPB)	
Dodecyl Pyridium bromide (DPB)	
Sodium dodecyl sulfate (SDS)	Alumina [39,41,66,67,69,70]
Igepal Co-660	Fumed silica [65]
Dodecyl Pyridium chloride (DPC)	Rutile (TiO_2) [40]
Sodium p-3 nonyl benzene sulfonate (SNBS)	
4-C_{11} paraxylene sulfonate	Alumina [42]
Cetyl trimethylammonium bromide (CTAB)	Cellulose [13]
Triton X-100 (TX-100)	Cellulose [44]

aggregate of the surfactant molecules on the solid surface. These surface aggregates are known as 'hemimicelles' [52]; which from beyond a critical concentration below the CMC, and is known as critical hemimicellar concentration (HMC). Hemimicellization was first hypothesized (for the adsorption of dodecylammonium ions on quartz) by Gaudin and Ferstenau [52]; later by others [35,36,41,51,53,71,72]. They have mentioned that the forces causing ionic association on the solid surface will be same as those operating in the bulk. Because of the high surface charge, the dodecylammonium ions must necessarily be oriented with the charged head towards the surface and with tail striking out into the liquid. This type of adsorption is termed as 'head on' adsorption [40]. Then the associative van der Waals force in the chains will be from hemimicelle. Mane et al. [73] have first reported the direct AFM imaging of 'hemimicelle' on graphite surface using cationic surfactant (CTAB), shown in Fig. 6. Gao et al. [53] have proposed a simple empirical equation to calculate the average aggregation number of the hemimicelle, n_{hm}, is given below

$$n_{hm} = \frac{\Gamma_{\infty}}{\Gamma_{hm}}. \tag{10}$$

Where Γ_{∞} and Γ_{hm} are the amounts adsorbed at saturation and HMC, respectively. Table 2 shows the reported hemimicellar aggregation number and the standard free energy change in Hemimicellization in different studies.

The effect of added salt (NaBr and NaCl) on adsorption of TPB and TPC on silica increases the packing of surfactant molecules as a result increases in aggregation number. Chandar et al. [41] have experimentally measured the hemimicellar aggregation number for adsorption of sodium dodecylsulfate (SDS) at alumina–water interface using fluorescence probe. They have found the aggregation number is 121–128 in region II and 166–356 in region III. From the table it is observed that alumina shows higher aggregation number. Since, negatively charged surfactant strongly adsorbed on positively charged alumina at pH 6.5. The aggregation numbers at different regions are shown in Fig. 7. In region II when the surface is positively charged, relatively uniform aggregates (120–130) are measured on the surface. Adsorption in this region occurs by increasing the number of aggregates on the positive sites of the particle. When the positive charge on the mineral is neutralized, the energetic situation favours the growth of existing aggregates rather than the formation of new aggregates. Thus in region III size of aggregates increases

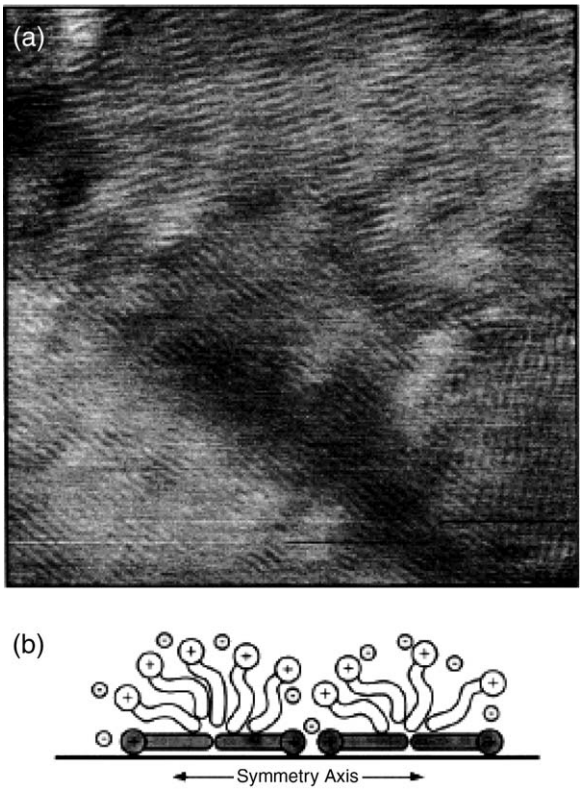

Fig. 6. (a) Adsorption CTAB on graphite at a solution concentration of ~ 0.8 mM. An AFM image obtained in non-contact mode using double layer forces between tip and sample. Image size 240 × 240 nm^2, z range 1.2 nm. The adsorbed structure is imaged as strips which are spaced 4.2 ± 0.04 nm apart (about twice the length of the adsorbed surfactant) organized into two-dimensional domains in which all the strips are parallel. (b) Proposed structure of hemicylindrical hemimicelles on the graphite surface. The bottom molecules (shaded) are probably bound epitaxially by the graphite surface, while the rest of the hemimicelle is more dynamic. Reproduced with permission from Ref. [73].

Table 2
Hemimicellar aggregation numbers of different systems

Surfactant	Medium	Adsorbent	Aggregation Number	$-\Delta G^0_{hm}/n_{hm}$ For 1 mol of surfactant (KJ)
DPB	Water	Silica gel	12 [53]	11.9 [72]
TPB	Water	Silica gel	13 [53]	13.8 [72]
	0.01 M NaBr		18	16.7
	0.01 M NaCl		14	15.3
	0.5 M C_2H_5OH		7	13.0
	0.1 M C_4H_9OH		7	13.5
	0.5 M C_4H_9OH		3	
TPC	Water	Silica gel	6 [53]	12.2 [72]
	0.01 M NaBr		14	16.4
	0.01 M NaCl		10	14.1
	0.01 M Urea		7	12.1
SDS	0.1M KCl, pH = 6.5	Alumina	121–128 [41] (region-II) 166–356 (region-III)	
C_{16}TAB	0.001 M KCl	PTFE	7 [51]	18.4 [51]
			6	17.1
C_{14}TAB			7	15.1
C_{12}TAB			4	14.8
CPC			4	14.4
DPC				
C_{16}TAB	0.001 M KCl	Polystyrene	8 [71]	19.2 [71]
			7	
		PTFE		18.4

significantly with adsorption density (166–356). The aggregation number in the different regions decreases with decreasing the surfactant chain length [60]. The bulk concentration of the surfactants at which transition of the regions occur is inversely proportional to the alkyl chain length of the surfactant molecule [33,60]. Fig. 8 shows the effect of chain length on hemimicellar aggregation number and region transition. Hemimicellar equilibrium constant and free energy also can be calculated using following equations [72]:

$$K_{hm} = \frac{\Gamma_\infty - \Gamma_{hm}}{C^{n_{hm}-1}(n_{hm}\Gamma_{hm} - \Gamma_\infty)}, \tag{11}$$

$$-\Delta G^0_{hm} = RT\ln K_{hm}, \tag{12}$$

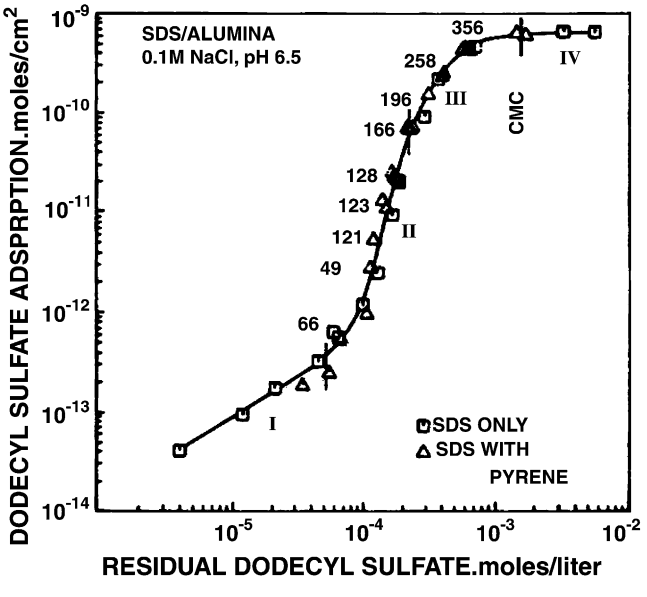

Fig. 7. Surfactant aggregation numbers as function of adsorption density (average aggregation number at each adsorption point shown along isotherm). Reproduced with permission from Ref. [41].

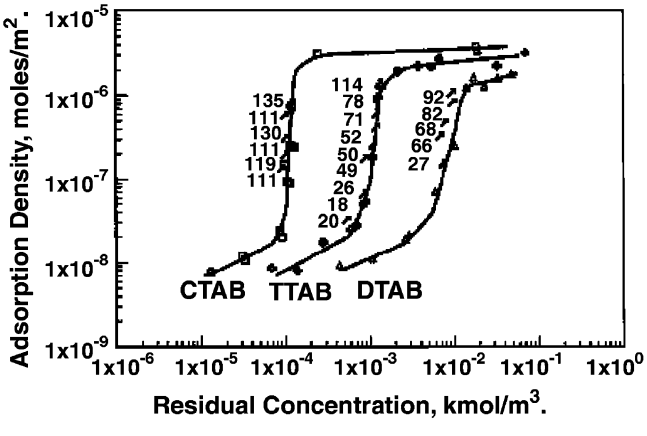

Fig. 8. Hemimicellar aggregation numbers of alkyltrimethylammonium bromide of three different chain lengths [CTAB (C_{16}), TTAB (C_{14}), DTAB (C_{10})] on alumina at pH 10. Reproduced with permission from Ref. [60].

where K_{hm} is the equilibrium constant and ΔG^0_{hm} is the standard free energy change for Hemimicellization.

In region III, there occurs a slowdown of new surface cluster formation and hence there is a reduction in the slope of isotherm. Ideally, the adsorption is expected to remain unchanged beyond the CMC (region IV) since the concentration of monomer does not increase beyond CMC and the micelles formed do not adsorb on the surface [14].

The observation of a maximum in region IV has drawn attention to some researchers and attempts have been made to explain this occurrence. The adsorption mechanism in region IV is not well understood. Presence of trace surface-active impurities in the surfactant sample has been attributed to the occurrence of this maximum. These would be adsorbed below the CMC but would be solubilised in the micelles above the CMC [18,49].

Trogus et al. [28] showed theoretically the presence of adsorption maximum and minimum using binary surfactant mixture and the Henry's law adsorption model. They also showed experimentally the adsorption C_{12} alkyl benzene sulfonate on Bera sandstone and Silica exhibits both adsorption maximum and minimum. Arnebrant et al. [29] observed the maximum in adsorption isotherm of SDS on chromium surfaces studied by in situ ellipsometry. In some of the cases reported in the literature, additional surfactant purification was found to decrease the amplitude of the adsorption maximum but could not completely eliminate it [29].

In another explanation, it is stated that, ionic strength of the solution reduces the electrical repulsion between adsorbed ions and the repulsive interaction becomes less than the van der Waal's attraction between the paraffin chains, leading to the formation of surface micelles. Desorption of both simple monomer ions and surface micelles occur on collision of micelles in solution with the adsorbing surface and thus decreasing the amount of adsorption on the surface [27].

Sexsmith and White [48] have explained the adsorption maxima using the principle of mass action of micellisation and the total mole balance equations. The equilibrium among counter ions, anionic or cationic surfactants and micelles can be shown to result in a decrease in the monomer concentration with increasing total concentration above the CMC. They write the mass action equation considering ideal solution as:

$$K = \frac{C_M}{C_Q^n C_x^{m_Q}}, \tag{13}$$

where K is an equilibrium constant, C_M molar concentration of micelle, C_Q and C_x are the monomer concentration of counter ion and surfactant, respectively, n and m_Q are the micellar aggregation number and number of counter ion per micelle, respectively. The conservation of total solute, C_T, present are expressed as follows:

$$C_T = nC_M + C_Q = m_Q C_M + C_x. \tag{14}$$

The equation can be solved for C_Q as a function of C_T and a maximum in C_Q will occur at the CMC if $n > m_Q \geq 2$. Thus, if one assumes that adsorption depends on the monomer concentration, the adsorption maximum occurs because the monomer concentration exhibits a maximum. The observation of maximum in the case of cotton surface has been attributed to the presence of wax, which gets solubilized beyond CMC [26].

In our own study, the adsorption sodium dodecylbenzenesulfonate on filter paper surface shows maximum in adsorption [44,74]. It was explained that the maximum is due to the presence of lower chain length surfactant molecules (higher CMC surfactants) as impurities. Lower chain surfactants are adsorbed to a less extent on the solid surface than the higher chain surfactants. If there is a solution of binary mixture of different chain length, one long (L) and the other short (S) then, the CMC of the mixed solution will be [75],

$$\frac{1}{\mathrm{CMC_{Mix}}} = \frac{\alpha_L}{f_L \mathrm{CMC}_L} + \frac{\alpha_S}{f_S \mathrm{CMC}_S}, \tag{15}$$

$\mathrm{CMC_{Mix}}$ is the CMC of the mixed solution, f is the activity coefficient of surfactant in the mixed micelle, equal to one for ideal system, α is the mole fraction of surfactant in total surfactant. The subscripts L and S represent long and short chain surfactant molecules, respectively, for simplicity. Below the $\mathrm{CMC_{Mix}}$ ($C_T \leq \mathrm{CMC_{Mix}}$) the monomer concentration of long chain will be,

$$C_L = \alpha_L C_T. \tag{16}$$

Above the CMC of the mixture ($C_T \geq \mathrm{CMC_{Mix}}$) monomer concentration of long chain in the bulk can be written as [75],

$$C_L = y_L \mathrm{CMC}_L, \tag{17}$$

$$C_S = (1 - y_L)\mathrm{CMC}_S. \tag{17a}$$

Micellar mole fraction of long chain component can be written as,

$$y_L = \frac{C_L}{\mathrm{CMC}_L} = \frac{(\alpha_L C_T - C_L)}{C_T - C_L - C_S}. \tag{18}$$

By eliminating C_S from Eq. (18), we get the concentration of monomer of long chain component above the mixed CMC [76,77],

$$C_L = \frac{-(C_T - \Delta) + \left\{(C_T - \Delta)^2 + 4\alpha_L C_T \Delta\right\}^{\frac{1}{2}}}{2\left(\frac{\Delta}{\mathrm{CMC}_L}\right)}, \tag{19}$$

$$C_L + C_S = \mathrm{CMC_{Mix}}, \tag{20}$$

where $\Delta = CMC_S - CMC_L$, C_T is the total surfactant concentration, y_L is the mole fraction of long chain component in mixed micelle. Fig. 9 shows the plot of C_T vs. C_L, C_S for a binary mixture of surfactants assuming 80% long chain and 20% short chain surfactant. Where the long chain surfactant has CMC of 1 mM, short chain has 10 mM. With the increase in the C_T above the mixed CMC of the mixture, monomer concentration of long chain component decreases and that of short chain increases. As micelles do not adsorb and short chain surfactants are less adsorbed, there will be a decrease in the amount of adsorption at the solid surface. Therefore, it was concluded that the existence of a maximum at around CMC in adsorption isotherm is due to the presence of short chain surfactant molecules. It is important to mention that the 'impurity' of the surfactant supply will not, in this case, show the minimum in a surface tension–concentration plot as this minimum is generated by a hydrophobic impurities which cannot self-assemble (i.e. does not form micelle on its own). In addition, to produce a minimum, the impurity must be more surface-active than the major component and be solubilised in the micelles of the major component. Thus, the absence of minima is necessary but not sufficient criterion of purity of surface-active agents [78]. Adsorption isotherms of TX-100 and SDS from their mixture on the filter paper surface were carried out to test the effects of bulk mixed micelle formation on adsorption at the solid–liquid interface [13]. In this case, TX-100 and SDS have the different CMC's and both the compounds form micelles individually. No surface tension minimum was observed in the SDS-TX-100 mixed surfactant system. Fig. 10a and b show the adsorption isotherm of TX-100 and NaDBS from their 80:20 and 70:30 mixtures, respectively. In both the cases, TX-100 isotherms show maximum adsorption nearer to concentration of mixed CMC and SDS isotherms show increasing amount adsorbed above the mixed CMC of the solution.

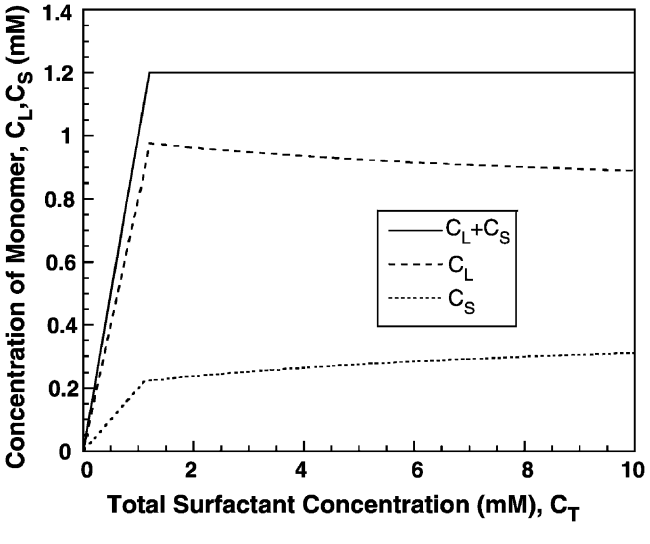

Fig. 9. Plot of total surfactant concentration vs. monomer concentrations, assuming binary surfactant system of ideal mixed micelle. $CMC_L = 1$ mM, $CMC_S = 10$ mM, $CMC_{Mix} = 1.2$, $\alpha_L = 0.8$, $\alpha_L + \alpha_S = 1$. Reproduced with permission from Ref. [13].

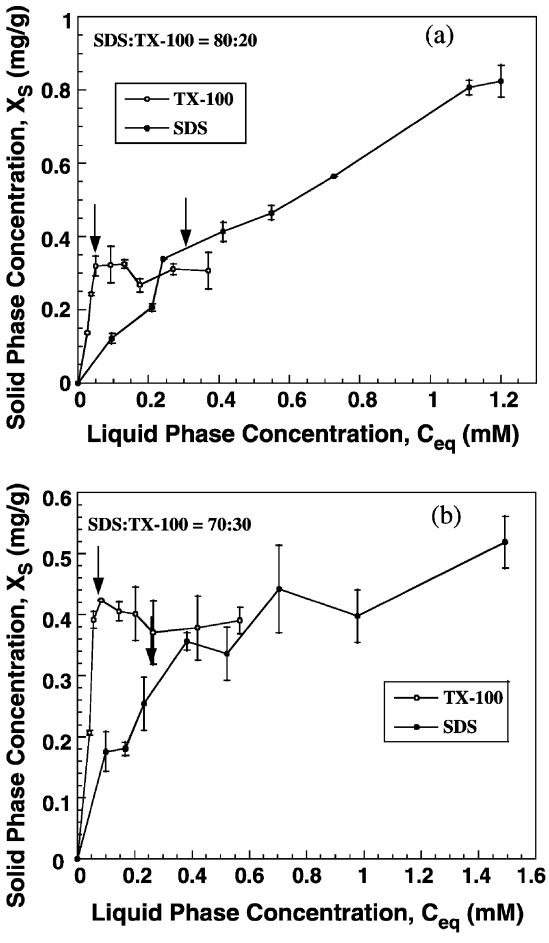

Fig. 10. (a) Adsorption isotherms of SDS and TX-100 from their 80:20 mixtures. (b) Adsorption isotherms of SDS and TX-100 from their 70:30 mixtures. Arrow indicates the CMC of surfactant in the mixture. Reproduced with permission from Ref. [13].

3.1.6. Influence of surfactant hydrocarbon chain length

With the increasing hydrocarbon chain length of the surfactant the surfactant molecules become more hydrophobic, which leads to the change in bulk properties of the solution. As a general rule, in aqueous medium, the greater the 'dissimilarity' between the surfactant and solvent, the greater the aggregation number [4]. As a result, surfactants with longer hydrocarbon chains have a much greater driving force for the aggregation, and thus dramatically reduce the solution CMC.

Chain length is also an important factor in determining the adsorption behaviour of a surfactant. There have been studies on effect of surfactant chain length on surfactant adsorption [36,50,60,62,68,79,80]. The effect of chain length on the adsorption isotherm is shown in Fig. 8. An increase in chain length is considered to decrease the Gibbs free energies of the micellisation and hemimicelli-

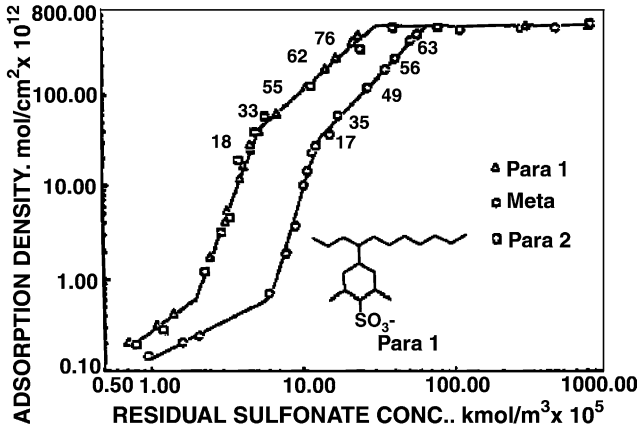

Fig. 11. Influence of functional groups of alkylxylene sulfonates on alumina. Reproduced with permission from Ref. [69].

zation process resulting in a shift of CMC and HMC toward lower concentrations. Addition of a CH_2 group to the chain is known to decrease the CMC and HMC by a factor of 3 (Traube's rule) [60]. The shifting of the isotherm to lower concentrations for longer chained surfactants is a result of increased hydrophobicity imparted by longer tail groups. At the solid–aqueous interface, hydrophobic interactions may exist between the surfactant and the surface, and also laterally between the adsorbed surfactants.

3.1.7. Influence of functional group

The structure of the adsorbed layer depends on the packing of the molecules, which in turn depends on the mutual repulsion, and steric constrains among adsorbate species [81]. Adsorption isotherms of 5-(4-undecyl)-2, 4-xylenesulfonate (Meta), 4-(4-undecyl)-3, 5-xylenesulfonate (Para-1) and 4-(4-undecyl)-2, 5-xylenesulfonate (Para-2) on alumina from water are shown in Fig. 11. The adsorption isotherm and hemimicellar aggregation numbers of the two paraxylene sulfonates are similar. However, at higher adsorption densities, the aggregation number of the metaxylenesulfonate is lower than that of the paraxylenesulfonate [69]. This suggests steric hindrance due to the position of functional groups on the aromatic ring of the alkylxylene sulfonate is important in packing of the surfactant molecules in the adsorbed layer.

3.1.8. Influence of electrolyte

The effect of electrolyte on the adsorption of surfactant at the solid–liquid interface have been studied [13,21,40,44,82,83]. It is shown that the presence of electrolyte enhances the adsorption of anionic surfactant on a negatively charged solid surface. The effective ness of valency of the counter ion in the adsorption enhancement of anionic surfactant onto negatively charged cellulose surface follows the *Schulze-Hardy* rule [44].

Koopal et al. [40] have studied the effect of ionic strength on the adsorption of anionic and cationic surfactant onto a oppositely charged solid surface. They observed the initial part of the isotherm, Regions I and II, adsorption occur at lower concentrations when the electrolyte concentration is low. The observations are shown in Fig. 12. Also, an increase in ionic strength of the bulk medium causes a screening of the coulombic attraction between the head group and surface, leading to a decrease in adsorption. Adsorption in the upper portion of region III is increased by raising the ionic strength, which indicates a reduction in mutual head group repulsion.

3.1.9. Influence of temperature

It has been observed that an increase in temperature leads to considerable decrease in the maximum quantity adsorbtion of ionic surfactants [21,22,84]. The lower the temperature, higher the maximum adsorbed. Meader and Fries [21], and Fava and Eyring [22] have studied the effect of temperature on adsorption of alkylbenzene sulfonate on cotton. Pavan et al. [84] have studied the temperature effect on adsorption of SDS on clay. This decrease in maximum adsorbed at higher temperature is expected as an increase in the kinetic energy of the species. Consequently, there is an increase in the entropy of the system, which results in a decrease of aggregate organization on the surface of the adsorbent [84].

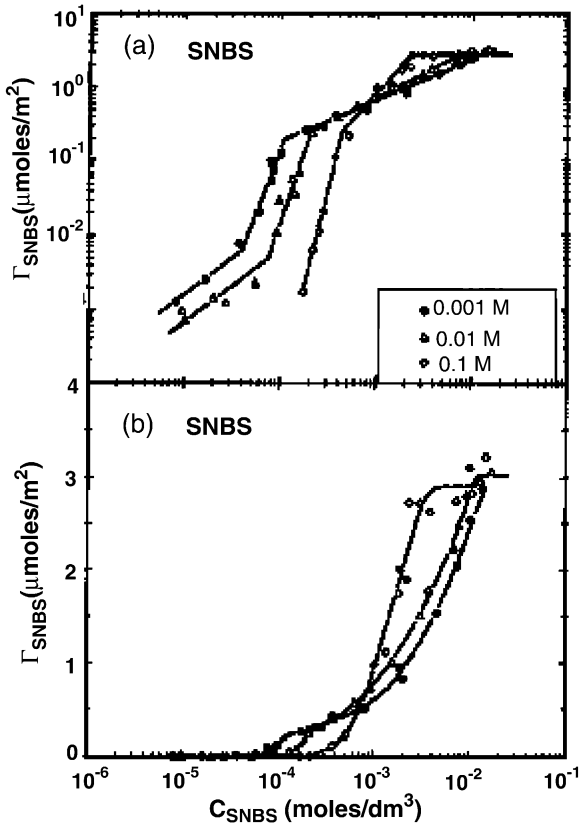

Fig. 12. Experimental isotherms of SNBS (sodium p-3-nonylbenzene sulfonate) on rutile at several electrolyte concentrations as indicated. The data are shown on both log–log (a) and lin–log (b) scales. Reproduced with permission from Ref. [40].

3.2. Adsorption of non-ionic surfactant

The adsorption of non-ionic surfactants on the solid–liquid interface has not been studied as extensively as the ionic surfactants [16,19,82,85–100]. The adsorption isotherms of non-ionic surfactants are generally Langmurian or L2 [101], like those of most other highly surface-active solutes adsorbing from the dilute solution. However, the isotherms are often the stepped L4 types of Langmuir isotherm [102] rather than simple L2 type.

Non-ionic surfactants are physically adsorbed rather than electrostatically or chemisorbed. However, they differ from many other surfactant in that, quite small changes in concentration, temperature, or molecular structure of the adsorbent can have a large effect on the adsorption. This is due to adsorbate–adsorbate and adsorbate–solvent interactions, which causes surfactant aggregation in bulk solution and which leads to change in orientation and packing of surfactant at the surface. Fig. 13a shows a general scheme of the most likely orientation changes undergo in the adsorption of non-ionic surfactants from solution onto solid surface and Fig. 13b shows three adsorption isotherms corresponding to the different adsorption sequences shown in Fig. 13a [101].

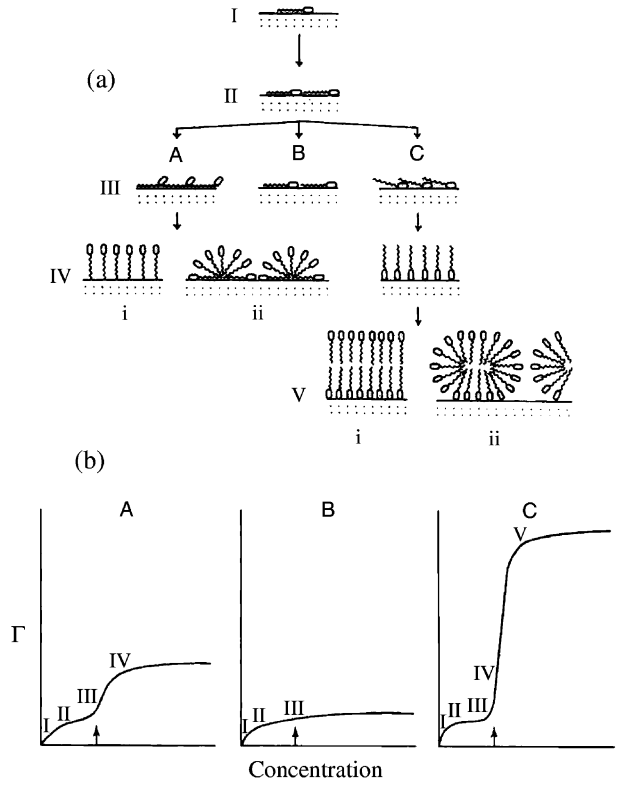

Fig. 13. (a) Adsorption of non-ionic surfactant, showing the orientation of surfactant molecules at the surface. *I–V* are the successive stages of adsorption. Reproduced with permission from Ref. [101]. (b) Adsorption isotherms corresponding to the three adsorption sequences shown in 2.4 (a) *I–V*, indicating the different orientations; CMC is indicated by an arrow. Reproduced with permission from Ref. [101].

In the first stage of the adsorption (Fig. 13a I) the surfactant is adsorbing on a surface where there are very few molecules which are adsorbed obeying Henry's law and because the molecules are far away from each other adsorbate–adsorbate interactions are negligible. Adsorption in this region occurs because of van der Waals interaction, and, therefore, it is mainly determined by the hydrophobic moiety of the surfactant. The second region (Fig. 13a II) is accompanied by gradual decrease in the slope of the adsorption isotherm due to saturation of monolayer.

The subsequent stages of adsorption are sudden increasing amount adsorbed dominated by adsorbate–adsorbate interactions, although it is the adsorbate–adsorbent interaction that initially determines how the adsorption progresses when stage II is complete. The adsorbate–adsorbate interaction depends on the nature of the adsorbent and on the hydrophilic–lipophilic balance (HLB) in the surfactant. When the hydrophilic group is weekly adsorbed (when adsorbent is hydrophobic and hydrophilic group of surfactant is short), it will be displaced from the surface by the alkyl chains of the adjacent molecules (Fig. 13a IIIA). However, if there is a strong attraction between the hydrophilic group and the surface with hydrophilic adsorbent like silica or oxides, the alkyl chain is displaced (Fig. 13a IIIC). The intermediate situation when neither type of displacement is favoured and the surfactant then remain flat on the surface (Fig. 13a IIIB).

Finally, in region IV the adsorption approaches a plateau above the CMC, there will be a tendency for the alkyl chains of the adsorbed molecules to aggregate (hemimicelle). This will cause the molecules to become vertically oriented and there will be a large increase in adsorption. This occurs for the hydrophobic adsorbent. Fig. 13a IVC shows the case of adsorption of non-ionic surfactant on hydrophilic solid.

3.2.1. Influence of molecular structure

The molecular structure of the surfactant influences the shape of the isotherm in various ways. Within a homologous series it is found that increasing length of the hydrocarbon chain generally increases the magnitude of adsorption, Γ_{max}, at the plateau and diminishes with the increasing size of the hydrophilic head group on the hydrophobic solid [85]. Partyka et al. [19] have found that rate of adsorption of series of ethylene oxide (EO) alkylphenol surfactant on the silica gel increases with increase in the chain length of hydrophilic group (EO) is shown in Fig. 14. For the adsorption isotherm with increasing chain length of EO group the amount adsorbed at the plateau decreases. Similar observation was found by Portet et al. [89] in study of the effect of chain length of hydrophilic group on adsorption. This effect can be attributed to the increase in the aqueous solubility of surfactant monomers and the corresponding reduction in affinity for hydrophobic surfaces. In addition, the area occupied by surfactant monomers in the adsorbed state becomes larger as the length of the EO chain increases.

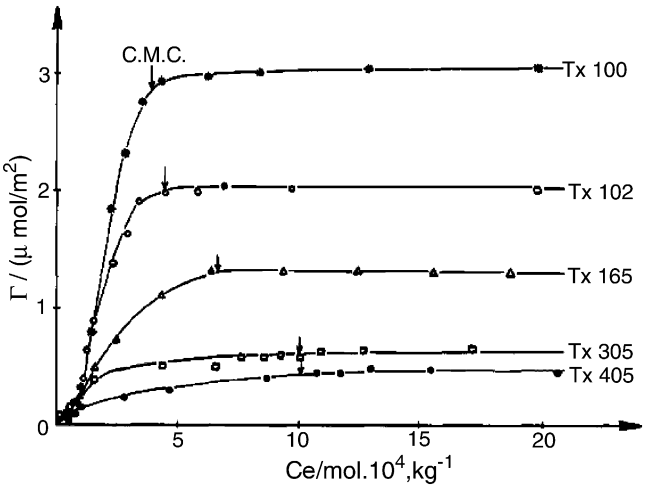

Fig. 14. Experimental adsorption isotherms of the oxyethylene octylphenol series on Spherosil at 20 °C. The order of EO group is TX-100 (9–10) <TX-102 (12–13) <TX-165 (16) <TX-305 (30) <TX-405 (40). Reproduced with permission from Ref. [19].

3.2.2. Influence of temperature

The adsorption of non-ionic surfactant on solid surface in general, increases with increasing temperature [19,85]. Corkill et al. [85] have studied the effect of temperature on adsorption of C_8E_3 and C_8E_6 on carbon black. They found in both the cases, the amount of adsorption increases with increasing temperature but the effect is strong in the case of C_8E_3. Partyka et al. [19] have found the adsorption of the homologous series of oxyethylene alkyl phenol the quantity Γ_{max}, the amount adsorbed at the plateau of the isotherm varies linearly with the temperature. However, adsorption of the surfactants increased with increasing temperature. This could not have been predicted from the calorimetric measurements and is not seen in physical adsorption from single component phases, i.e. gas on solid. Corkill et al. [85] suggested that the adsorbing species is actually the solvated surfactant molecule, which is essentially different at each temperature because the surfactant–solvent interaction, like polyethoxylated surfactants which are very sensitive to temperature. Increasing temperature gradually desolvates the head group, making it less hydrophilic and more compact, and thus increases the surface activity and saturation adsorption values.

3.2.3. Influence of electrolyte

Electrolytes can alter the solubility, surface activity, aggregation properties of non-ionic surfactant, and thereby it may have an effect on adsorption at the solid/liquid interface [4,101]. Thus, an electrolyte that 'salts out' a surfactant would probably increase its adsorption. Denoyel and Rouquerol [103] found that the presence of NaCl shifts plateau position of TX-100 adsorbed on quartz towards lower equilibrium concentrations, which means that there is a decrease of the CMC. At the same time, these authors observed a rise in adsorption at the plateau. They explained this behaviour to an increase in lateral interactions between the polar chains, when salinity increases. Similar observation was also found for the adsorption of non-ionic surfactant on silica gel [19,88]. It has been shown that pH has some influence on the adsorption of non-ionic surfactants on the surfaces with hydroxyl groups [103]. At neutral pH, adsorption of TX-100 on quartz is low but it is increased at lower pH. This effect was attributed to the hydrogen bonding between polar chain of the surfactant and the silanol groups of the surface. Nevskaia et al. [82] have studied the effect of added NaCl and $CaCl_2$ on adsorption of TX-100 on three different quartz (increasing order of hydroxyl group, QA>QB>QC), kaolin and dolomite. Basically, three different observations have been found when NaCl is added. Fig. 15 shows the amount of adsorption of TX-100 decreases when NaCl is added to the QA sample; the amount increases on QB and kaolin samples; no alteration is observed for QC and dolomite samples. They explained that the decreasing adsorption was due to the strong adsorption of inorganic ions on the polar surface and the resulting displacement of the non-ionic surfactant molecules.

3.3. Self-assembly and mechanism of adsorption by AFM study

In the past few years, the atomic force microscopy (AFM) has been used directly to image the adsorbed surfactant at the solid–liquid interface. In general, AFM has been used with contact mode (where the tip will touch

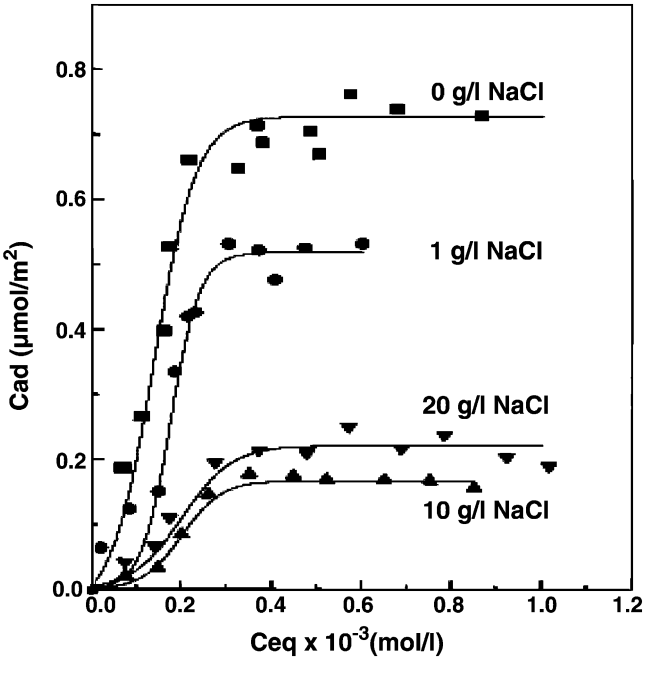

Fig. 15. Adsorption isotherms of TX-100 at 298 K on the QA sample with different NaCl concentrations. Reproduced with permission from Ref. [82].

the substrate) for the imaging of hard surfaces but in appropriate for the imaging of the adsorbed surfactant layers. Surfactant aggregates are fragile, so hard contact measurements will destroy the adsorbed morphology. In the non-contact mode, the repulsive electrical double layer force associated with the adsorbed species is used to generate information about the adsorbed layer. The first direct imaging of CTAB on the cleavage plane of highly ordered pyrolytic graphite [73,10]. Mainly the electrical double layer repulsion was used to image a cationic surfactant at the graphite/solution interface. The graphite is frequently used substrate for the AFM, because it is atomically smooth crystalline from which is required for the AFM study, and graphon, a form of particular graphite is often used as hydrophobic adsorbate [59]. Different surfactant aggregate morphologies have been studied on mica for cationic [105–107], gemini [108], zwitterionic surfactants [109]; on graphite for anionic [110–112], cationic [73,104], non-ionic [113–115], zwitterionic surfactants [111]; on silica for cationic [116–118], non-ionic [115], zwitterionic surfactants [109].

Fleming and Wanless [110] have schematically represented the soft-imaging of these hemicylindrical adsorbed structure by AFM in Fig. 16. It is shown in the figure that the scanning probe 'rides' across the top of hemicylindrical aggregates, deflecting only slightly in between them. The high normal resolution of the microscope registers this deflection (of the order of 0.2 nm) easily, and the periodical image of aggregates is a deflection map of the surface of the adsorbate.

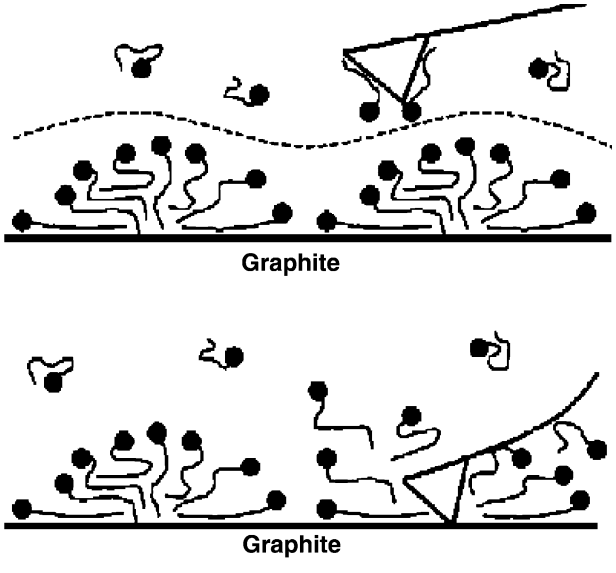

Fig. 16. A schematic showing the interaction between the AFM probe and the adsorbed layer. The upper section illustrates soft-imaging mode where the undulating dotted line indicates the typical deflection of the cantilever during a single scan line when scanning on the adsorbed layer. The lower section illustrates contact mode imaging in which the substrate is imaged. Note that the tip is undersized in order to show both the tip and cantilever on the molecular scale. Reproduced with permission from Ref. [110].

3.3.1. Time dependency of adsorbed structure

Attractive and repulsive force was measured with time during adsorption and desorption of CTACl on silica [116]. Immediately (approx. 20 s) after exposure of the silica to a 2.0 mM solution of CTACl, a large repulsive and adhesive force was measured. This is indicated the presence of bilayer surfactant. When the cell was rinsed with water the repulsive force was replaced by the attractive force and even larger adhesive force. Also, there was no longer existence of surface micelle. This shows that the surfactants that cause the changes of reversal of the surface are easy to desorb. The molecules that neutralize the charge take more time to desorb. The molecules held by stronger electrostatic forces take longer time to desorb than the molecule held by weaker hydrophobic interactions. They also found that when the adsorption time was short (10 min), the adhesion decreases to <1 nN in approximately 20 min. When the adsorption time was long (20 h) the adhesion did not decrease below 1 nN until approximately 35 h.

3.3.2. Influence of counter ion on adsorbed structure

Influence of counterion on adsorbed morphology of surfactant layer has also been studied [112,117,118]. Wanless and Ducker [111] have studied the effect of ionic strength on the aggregate spacing. Fig. 17a shows the AFM image of adsorbed SDS structure from 2.8 mM concentration on graphite and Fig. 17b shows the structure in presence of 20 mM NaCl. The structure is much more clear and the period is smaller in presence of 20 mM NaCl. Fig. 17c shows a plot of the period as a function of solution Debye length. The period decreases linearly with Debye length of the solution. So, they suggested that the period is controlled by the charged interaction between the aggregates. Wanless and Ducker [112] observed the addition of divalent ion, Ca^{++}, Mg^{++}, Mn^{++} to the adsorption of SDS on graphite does not cause a change in the shape of aggregates. The divalent ions do lower the surface aggregation concentration and increase the adsorption density. Velegol et al. [117] observed in the absence and presence of 10 mM KCl CTAB morphology changes from short rods to worm like when the concentration was increased from 0.9 to $10\times$ cmc. The peak-to-peak distance between CTAB aggregates was 10 ± 2 nm at $10\times$ cmc and 13 ± 2 $0.9\times$ cmc, but there was no significant changes between the peak-to-peak distance in the absence or presence of 10 mM KCl. Subramaniam et al. [118] have studied the effect of counterion on the shape changes of CTA^+ micelle on silica surface. They rationalized the effect on the basis of hard/soft (unpolarizable/polarizable) nature of the ions. Addition of $S_2O_3^{2-}$ or CS_3^{2-}, HS^-/S^{2-} transfer spherical micelles to cylindrical micelle. Generally, the molecules with a soft negative atom effect the transformation, because the soft atoms prefer to bind with the quaternary ammonium head group of CTA^+ rather than

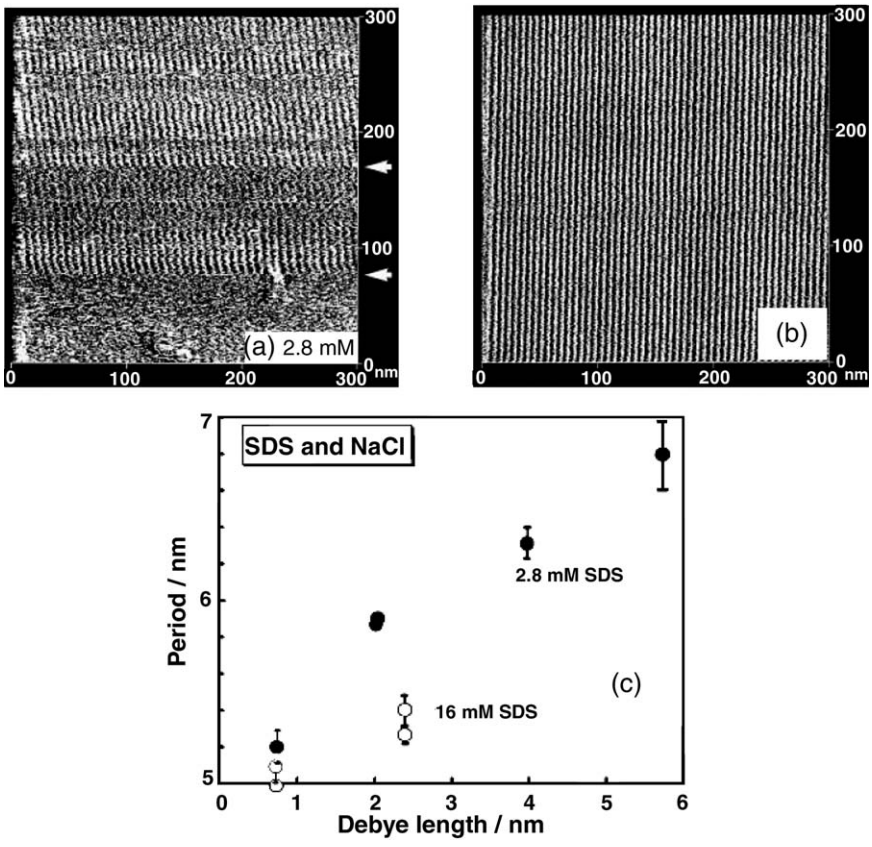

Fig. 17. (a) AFM images showing the one-dimensional periodicity of adsorbed SDS on graphite in aqueous SDS solutions at 2.8 mM SDS. (b) Structure of adsorbed surfactant in 2.8 mM SDS and 20 mM NaCl showing the period is smaller. (c) Effect of NaCl on adsorbate periodicity. The filled circles show the change in period for 2.8 mM SDS solutions. There is an approximately linear relationship between period and Debye length [and also with log (concentration)]. Some data for 16 mM SDS (open circles) are shown on the same figure. Reproduced with permission from Ref. [111].

water. This reduces the repulsive interaction between head groups and lowers the energy of the less curved cylindrical portion of the micelle.

4. Adsorption of mixed surfactant

Adsorption of more than one surfactant significantly enhances the efficiency of many interfacial properties compared to the adsorption of a single surfactant. Although the adsorption of single surfactants at solid–liquid interface has been investigated intensively, there have been only a few studies of mixed systems, in spite of their great importance [1,10,11,39,119–126]. Adsorption of surfactants from the mixed systems mainly depends on the solution properties of mixed surfactant system. Many researchers have studied the solution properties of mixed surfactant systems and the resulting adsorption.

4.1. Anionic–cationic surfactant mixture

Only a few reported studies are available on the adsorption from a solution of anionic–cationic mixed surfactant. Huang et al. [119] have studied the adsorption of cationic and anionic surfactants on silica from the mixture of anionic and cationic surfactants. They have found that the individual cationic surfactants can be strongly adsorbed onto the silica gel, but no significant adsorption of anionic surfactant can be detected. However, in the mixed systems, the adsorption amount of both the cationic and anionic surfactant ions is enhanced and the excess adsorption of cationic surface-active ions is exactly equal to the adsorption of anionic surface-active ions. From the observations, they assumed that the excess adsorption of cationic and anionic surface-active ions is in the form of ion pairs.

We have also studied the adsorption of anionic–cationic mixed surfactant system on the cellulose–water interface [127]. Fig. 18 shows the adsorption enhancement of anionic surfactant (NaDBS) in presence of cationic surfactant (CTAB) at the cellulose–water interface. The enhancements both in rate and amount are smaller compared to the pre-treated surfaces (if the cellulose surface was preadsorbed with the same concentration of CTAB and then adsorbed with only NaDBS). The main reason for this difference is because cationic and anionic surfactants, in mixture, form an ion pair and this behaves like surfactant with almost no

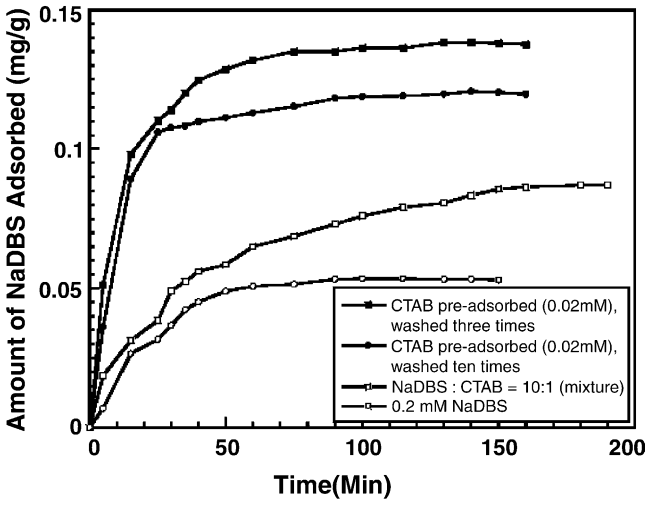

Fig. 18. Comparison of adsorption enhancement between NaDBS (0.2 mM), NaDBS/CTAB mixture (10:1 mole ratio) and NaDBS (0.2 mM) with pre-adsorbed filter paper in 0.02 mM CTAB solution. Reproduced with permission from Ref. [127].

charge and hence lesser adsorption than CTAB. The adsorption appears to be purely due to hydrophobic interactions.

4.2. Anionic–non-ionic surfactant mixture

Adsorption of anionic–non-ionic surfactant has been studied by many researchers at the solid–liquid interface [1,10,11,69,120–125]. Adsorption of anionic and non-ionic surfactants from their mixture on positively charged alumina [39,123,124] and kaolinite has been reported [125]. It is observed that adsorption of non-ionic surfactant is enhanced where non-ionic alone shows trace adsorption and adsorption of anionic surfactant slightly decreases. Another feature of adsorption isotherm is that with the increasing molar ratio of non-ionic surfactant the continuous shift of plateau of isotherm of anionic surfactant towards lower concentration and the Hemimicellization concentration of anionic surfactant also shifts towards lower concentration. Adsorption of non-ionic surfactant (TX-100) from the mixture of anionic–non-ionic surfactant on negatively charged silica gel shows the decreasing amount of adsorbed TX-100 above the CMC with increasing concentration of anionic surfactant and there is no change in isotherm below the CMC between mixed system and the pure TX-100 [121]. The decrease of limiting adsorption is greater at the same concentration of anionic surfactant with longer alkyl chain length. Somasundaran and Huang [1] have found that in the case of adsorption of anionic/non-ionic surfactant on kaolin, when the hydrocarbon chain length of non-ionic surfactant is equal or longer than that of anionic, isotherms of anionic surfactant do not change with changing the chain length of non-ionic surfactant. But, if the chain length of non-ionic surfactant is shorter than that of anionic, however, different isotherms of anionic surfactant are obtained due to less shielding of anionic surfactant. Fig. 19 shows the schematic presentation of the effect of non-ionic surfactant chain length on the adsorption of anionic surfactant from their mixture [1].

4.3. Cationic–non-ionic surfactant mixture

Adsorption of mixture of cationic and non-ionic surfactants on a negatively charged alumina [1,69,124], silica [128], limestone [129], teflon [130] and on kaolinite [125]. In case of adsorption of cationic and non-ionic surfactant on negatively charged alumina from their mixture, similar to anionic and non-ionic surfactant mixture onto positively charged solid, the adsorption of tetradecyl-trimethyl-ammonium chloride (TTAC) and pentadecylethoxylated-nonyl-phenol (NP-15) on alumina from their mixture have been studied [1]. The TTAC does adsorbed on negatively charged alumina (at pH = 10) but NP-15 does not adsorbed alone on the alumina. The adsorption behaviour depends upon the ratio of the two surfactants. Fig. 20 shows the adsorption isotherms of NP-15 from the TTAC-NP-15 mixture. With increasing the TTAC concentration of the mixtures, the adsorption of NP-15 is enhanced significantly, and the adsorption isotherms are shifted to lower concentration ranges. In case of adsorption of TTAC, the plateau adsorption decreases markedly upon the addition of non-ionic surfactant. This is attributed to the competition of the bulky non-ionic NP-15 with TTAC for the adsorption sites under saturated adsorption conditions. Desai and Dixit [130] also observed similar effects on teflon–water interface. Penfold et al. [128] found that the structure of bilayer formed at the hydrophilic silicon aqueous solution interface by the

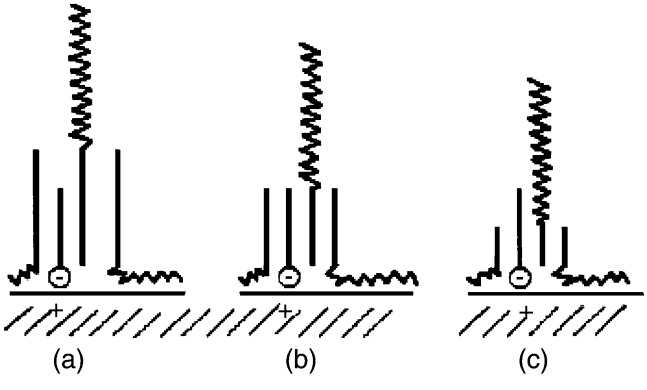

Fig. 19. Schematic presentation of the effect of non-ionic surfactant hydrocarbon chain length on the adsorption of the anionic sodium dodecyl sulfate (SDS). (a) Non-ionic surfactant hydrocarbon chains longer than that of SDS; (b) non-ionic surfactant hydrocarbon chain length equal to that of SDS; (c) non-ionic surfactant hydrocarbon chain length shorter than that of SDS, partially exposing SDS hydrocarbon chains to the aqueous solution or the hydrophilic ethoxyl chains of the non-ionic surfactant. Reproduced with permission from Ref. [1].

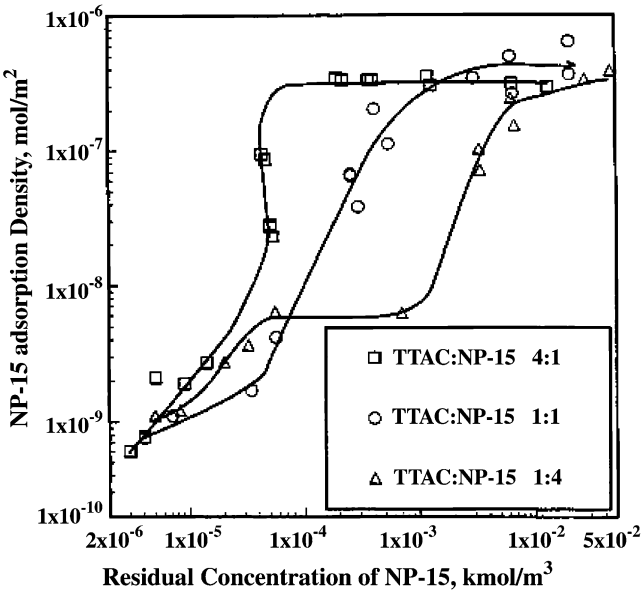

Fig. 20. Adsorption of pentadecylethoxylated-nonyl-phenol (NP-15) on alumina in the presence of varying amounts of tetradecyl-trimethyl-ammonium chloride (TTAC). pH 10.5, I.S. 0.03 M NaCl. Reproduced with permission from Ref. [1].

mixed cationic (C_{16}TAB)/non-ionic (hexaethylene glycol monodecyl ether, $C_{12}E_6$) surfactant mixture. The specular neutron reflection was used to determine the structure and composition of mixed surfactant layers adsorbed at the solid–liquid interface.

5. Concluding remarks

In this review, we have presented the adsorption of anionic, cationic, non-ionic and mixed surfactants at the hydrophilic solid–liquid interface. Special emphasis has been put on the kinetics and equilibrium studies of different surfactants. Different regions of adsorption isotherms are described in details. The major conclusions from this review are:

1. The kinetics of adsorption mainly depends on the nature of the adsorbent and the surfactant type. If the surfactant and the adsorbent are oppositely charged the rate of adsorption is very fast and the equilibrium time is also less. The rate of adsorption of non-ionic surfactant on the hydrophilic silica depends on the diffusion coefficient of the monomer and the thickness of the stagnant layer.
2. The nature of the adsorption isotherm of surfactant depends on the nature of the adsorbent and the type of the surfactant. Generally, adsorption of ionic surfactants onto oppositely charged solid surface show four-region isotherm.
3. The hemimicellar aggregation numbers at region II and III decreases with the decreasing chain length of the surfactants. The steric hindrance due to the position of the functional group in the surfactant also decreases the hemimicellar aggregation number.
4. In general, the region IV beyond the CMC, the adsorption isotherms show the plateau region. Sometimes for the mixed surfactant systems the region IV, show maximum. The maximum is due to the presence of different CMC surfactants present in the mixture. Generally, the lower CMC surfactants have the greater tendency to adsorb at the solid surface but above the CMC the monomer concentration of the lower CMC surfactants decrease due to formation of mixed micelle.
5. The adsorption of ionic surfactant on similarly charged solid surface enhanced in presence of electrolyte. The effectiveness of the valency of the counterion in the adsorption enhancement follows *Schulze-Hardy* rule.
6. The maximum amount adsorbed at the plateau for ionic surfactant decreases with increasing temperature.
7. Adsorption of non-ionic surfactants in a homologous series the magnitude of adsorption at the saturation increases by increasing the length of the hydrocarbon chain length. The magnitude of adsorption at the saturation decreases by increasing the chain length of the hydrophilic group. The rate of adsorption increases by increasing the chain length of the hydrophilic group.
8. The maximum amount adsorbed at the plateau for non-ionic surfactant decreases with the increasing temperature.
9. AFM studies of adsorbed surfactant show the surfactant molecules form hemicylindrical stripes of adsorbed structure at the solid–liquid interface. If the molecules are adsorbed by strong electrostatic attraction and if adsorbed for long time then it takes long time to desorb from the surface. The peak-to-peak distance between the surfactant aggregates decrease in presence of salt. The periods decrease linearly with the Debye length of the solution.
10. The adsorption of anionic surfactant onto a negatively charged surface is enhanced in presence of cationic surfactant due to formation of ion pairs. The enhancement of adsorption of anionic surfactant will be more if the solid surface is pre-treated with the cationic surfactant rather than mixing of anionic–cationic surfactant in the bulk. In the case of anionic–non-ionic mixed surfactant adsorption when the hydrocarbon chain of non-ionic surfactant is equal or longer than the anionic surfactant, the isotherm of anionic surfactant do not changes with changing the hydrocarbon chain length of the non-ionic surfactant. But, if the chain length of the non-ionic surfactant is shorter than that of anionic, different isotherms of anionic surfactant will be obtained due to less shielding of anionic surfactant.

Notations

C	Molar concentration of ion, k mole m^{-3}
C_{eq}	Equilibrium concentration, k mole m^{-3}
C_M	Molar concentration of micelle, k mole m^{-3}
C_Q	Monomer concentration of counter ion, k mole m^{-3}
C_T	Total concentration, k mole m^{-3}
C_L, C_S, C_x	Monomer concentration of surfactant, k mole m^{-3}
e	Electronic charge, C
E_{ads}	Electric field strength, J
F	Faraday constant, C $mole^{-1}$
f_L, f_S	Activity coefficient.
ΔG^0_{ads}	Free energy of adsorption, J
ΔG^0_{c-c}	Free energy for chain-chain interaction, J
ΔG^0_{chem}	Free energy for covalent bonding, J
ΔG^0_{coul}	Free energy for columbic interaction, J
ΔG^0_{dip}	Free energy for dipole interaction, J
ΔG^0_{elec}	Free energy for electrical interaction, J
ΔG^0_{H}	Free energy for hydrogen bonding, J
$\Delta G^0_{H_2O}$	Free energy for solvation, J
ΔG^0_{hm}	Standard free energy change for Hemimicellization, J
ΔG^0_{spec}	Free energy for non-electrical term, J
K	Equilibrium constant
k_B	Boltzmann constant, J K^{-1}
K_{hm}	Equilibrium constant for Hemimicellization
m_Q	Number of counter ion per micelle
n	Micellar aggregation number
n_{hm}	Hemimicellar aggregation number
r	Radius of the surfactant molecule, m
R	Gas constant, J K^{-1} $mole^{-1}$
T	Absolute temperature, K
x	Distance, m
X_S	Total solid phase concentration of surfactant (amount adsorbed), kg kg^{-1}
y_L	Micellar mole fraction
z	Valency of ion

Greek letters

α, α_L, α_S	Mole fraction of surfactants
δ	Stern layer thickness, nm
ε	Dielectric permittivity, C^2 J^{-1} m^{-1}
$\varepsilon_0\varepsilon_0$	Dielectric permittivity in vacuum, C^2 J^{-1} m^{-1}
Γ	Amount adsorbed at the interface, k. mole m^{-2}
Γ_{hm}	Amount adsorbed at HMC, kg kg^{-1}
Γ_∞	Amount adsorbed at saturation, kg kg^{-1}
κ	$(\text{Debye length})^{-1}$, nm^{-1}
μ	Dipole moment, C m
ψ	Electric potential, mV
ψ_δ	Electric potential at the stern plane, mV
ψ_0	Electric potential at the solid surface, mV
σ_δ	Charge density at δ, C m^{-2}
σ_0	Charge density at the surface, C m^{-2}

Abbreviations

CMC	Critical micellar concentration
CMC_{Mix}	Mixed CMC
CPC	Cetylpyridinium chloride
CTAB, $C_{16}TAB$	Cetyl trimethyl ammonium bromide
$C_{14}TAB$	Myristyl trimethyl ammonium bromide
$C_{12}TAB$	Dodecyl trimethyl ammonium bromide
DDAB	Dimethyldioctadecylammonium bromide
DPB	Dodecyl pyridinium bromide
DPC	Dodecyl pyridinium chloride
EO	Ethylene oxide
HLB	Hydrophilic lipophilic balance
HMC	Hemimicellar concentration
NaDBS	Sodium dodecylbenzenesulfonate
NP-15	Pentadecylethoxylated-nonyl phenol
PTFE	Polytetrafluoroethylene
SDS	Sodium dodecyl sulfate
SNBS	Sodium p-3 nonyl benzene sulfonate
TPB	Tetradecyl pyridinium bromide
TPC	Tetradecyl pyridinium chloride
TTAC	Tetradecyl trimethyl ammonium chloride

References

[1] P. Somasundaran, L. Huang, Adv. Colloid Interface Sci. 88 (2000) 179.
[2] A.P. Robertson, J.O. Leckie, J. Colloid Interface Sci. 188 (1997) 444.
[3] R.K. Iler, The Chemistry of Silica, Wiley, New York, 1979.
[4] M.J. Rosen, Surfactants and Interfacial Phenomena, Wiley-Interscience Publication, New York, 1978.
[5] J.C. Griffith, A.E. Alexander, J. Colloid Interface Sci. 25 (1967) 311.
[6] J.F. Scamehorn, J.F. Harwell, in: D.T. Wasan, M.E. Ginn, D.O. Shah (Eds.), Surfactants in Chemical/Process Engineering, Marcel Dekker, New York, 1988, Chapter 3.
[7] N.O.V. Sonntag, in: D.T. Wasan, M.E. Ginn, D.O. Shah (Eds.), Surfactants in Chemical/Process Engineering, Marcel Dekker, New York, 1988, Chapter 7.
[8] H.J.F. Gecol, J.F. Scamehorn, S.D. Christian, B.P. Grady, F. Riddell, Colloids Surf. A 189 (2001) 55.
[9] P.K. Kang, D.O. Shah, Langmuir 13 (1997) 1820.
[10] C. Ma, Y. Xia, Colloids Surf. 66 (1992) 215.
[11] C. Ma, Y. Xia, Colloids Surf. 68 (1992) 171.
[12] B.J. Palla, D.O. Shah, J. Colloid Interface Sci. 223 (2000) 102.
[13] S. Paria, C. Manohar, K.C. Khilar, J. Inst. Eng. Singapore (2003) 34, Chem. Eng. Issue 43.
[14] J. Brinck, B. Jönsson, F. Tiberg, Langmuir. 14 (1998) 1058.
[15] J. Brinck, B. Jönsson, F. Tiberg, Langmuir 14 (1998) 5863.
[16] F. Tiberg, J. Chem. Soc., Faraday Trans. 92 (1996) 531.
[17] F. Tiberg, B. Jönsson, B. Lindman, Langmuir 10 (1994) 3714.
[18] E.S. Pagac, D.C. Prieve, R.D. Tilton, Langmuir 14 (1998) 2333.
[19] S. Partyka, S. Zaini, M. Lindheimer, B. Brun, Colloids Surf. 12 (1984) 255.
[20] S.C. Biswas, D.K. Chattoraj, J. Colloid Interface Sci. 205 (1998) 12.
[21] A.L. Meader, B. Fries, Ind. Eng. Chem. 44 (1952) 1636.
[22] A. Fava, H. Eyring, J. Phys. Chem. 60 (1956) 890.
[23] S. Paria, C. Manohar, K.C. Khilar, Submitted.
[24] A. Gurses, M. Yalcin, M. Sozbilir, C. Dogar, Fuel Process. Technol. 81 (2003) 57.
[25] A. De Keizer, J. Lyklema, J. Colloid Interface Sci. 75 (1980) 171.

[26] M.E. Ginn, F.B. Kinney, J.C. Harris, J. Am. Oil Chem. Soc. 38 (1961) 138.
[27] R.D. Vold, N.H. Sivaramakrishnan, J. Phys. Chem. 62 (1958) 984.
[28] F.J. Trogus, R.S. Schechter, W.H. Wade, J. Colloid Interface Sci. 293 (1978) 70.
[29] T. Arnebrant, K. Bäckström, B. Jönsson, T. Nylander, J. Colloid Interface Sci. 128 (1989) 303.
[30] W.H. Keesom, R.L. Zelenka, C.J. Radke, J. Colloid Interface Sci. 125 (1988) 575.
[31] H.M. Rendall, A.L. Smith, L.A. Williams, J. Chem. Soc. Faraday Trans-1 75 (1979) 669.
[32] H.C. Evans, J. Colloid Sci. 13 (1958) 537.
[33] J.F. Scamehorn, R.S. Schechter, W.H. Wade, J. Colloid Interface Sci. 85 (1982) 463.
[34] J.F. Scamehorn, R.S. Schechter, W.H. Wade, J. Colloid Interface Sci. 85 (1982) 479.
[35] P. Somasundaran, D.W. Fuerstenau, J. Phys. Chem. 70 (1966) 90.
[36] P. Somasundaran, T.W. Healy, D.W. Fuerstenau, J. Phys. Chem. 68 (1964) 3562.
[37] B. Tamamushi, K. Tamaki, Trans. Faraday Soc. 55 (1959) 1007.
[38] C.E. Hoeft, R.L. Zollars, J. Colloid Interface Sci. 177 (1996) 171.
[39] W. Wang, J.C.T Kwak, Colloids Surf. A 156 (1999) 95.
[40] L.K. Koopal, E.M. Lee, M.R. Böhmer, J. Colloid Interface Sci. 170 (1995) 85.
[41] P. Chandar, P. Somasundaran, N.J. Turro, J. Colloid Interface Sci. 117 (1987) 31.
[42] N.P. Hankins, J.H. O'Haver, J.H. Harwell, Ind. Eng. Chem. Res. 35 (1996) 2844.
[43] O. Ofor, J. Colloid Interface Sci. 174 (1995) 345.
[44] S. Paria, C. Manohar, K.C. Khilar, Submitted.
[45] D.W. Fuerstenau, J. Colloid Interface Sci. 256 (2002) 79.
[46] S.C. Biswas, D.K. Chattoraj, Langmuir 13 (1997) 4505.
[47] F.H. Sexsmith, H.J. White, J. Colloid Sci. 14 (1959) 598.
[48] F.H. Sexsmith, H.J. White, J. Colloid Sci. 14 (1959) 630.
[49] E.M. Furst, E.S. Pagac, R.D. Tilton, Ind. Eng. Chem. Res. 35 (1996) 1566.
[50] P. Connor, R.H. Ottewill, J. Colloid Interface Sci. 37 (1971) 642.
[51] A.K. Vanjara, S.G. Dixit, J. Colloid Interface Sci. 177 (1996) 359.
[52] A.M. Gaudin, D.W. Fuerstenau, Trans. AIME 202 (1955) 958.
[53] Y. Gao, J. Du, T. Gu, J. Chem. Soc., Faraday Trans-1 83 (1987) 2671.
[54] N.K. Dimov, V.L. Kolev, P.A. Kralchevsky, L.G. Lyutov, G. Broze, A. Mehreteab, J. Colloid Interface Sci. 256 (2002) 23.
[55] J.J. Alder, P.K. Sing, A. Patist, Y.I. Rabinovich, D.O. Shah, B.M. Mudgil, Langmuir 16 (2000) 7255.
[56] N. Öztekin, S. İşçi, F.B. Erim, N. Güngör, Mater. Lett. 57 (2002) 684.
[57] E. Sabah, M. Turan, M.S. Celik, Water Res. 36 (2002) 3957.
[58] K. Esumi, Colloids Surf. A 176 (2001) 25.
[59] R. Atkin, V.S.J. Craig, E.J. Wanless, S. Biggs, Adv. Colloid Interface Sci. 103 (2003) 219.
[60] A. Fan, P. Somasundaran, N.J. Turro, Langmuir 13 (1997) 506.
[61] T.P. Goloub, L.K. Koopal, Langmuir 13 (1997) 673.
[62] J. Wang, B. Han, M. Dai, H. Yan, Z. Li, R.K. Thomas, J. Colloid Interface Sci. 213 (1999) 596.
[63] A.W. Adamson, A.P. Gast, Physical Chemistry of Surfaces, Wiley-Interscience, New York, 1997, Chapter-V.
[64] D.B. Hough, H.M. Rendall, in: G.D. Parfitt, C.H. Rochester (Eds.), Adsorption from Solution at the Solid/Liquid Interface, Academic Press, New York, 1983, p. 247, Chapter-6.
[65] J.H. Harwell, J.F. Scamehorn, in: K. Ogino, M. Abe (Eds.), Mixed Surfactant Systems, Marcel Dekker, New York, 1993, Chapter-9.
[66] J.H. Harwell, B.L. Roberts, J.F. Scamehorn, Colloids Surf. 32 (1988) 1.
[67] J.J. Lopatta, J.H. Harwell, J.F. Scamehorn, ACS Symposium Series 373, ACS, Washington, DC, 1988, Chapter-10.
[68] S. Chandar, D.W. Fuerstenau, D. Stigter, in: R.H. Ottewill, C.H. Rochester, A.L. Smith (Eds.), Adsorption from Solution, Academic Press, New York, 1983, p. 197.
[69] P. Somasundaran, S. Krishnakumar, Colloids Surf. A 123–124 (1997) 491.
[70] B.L. Roberts, J.F. Scamehorn, J.H. Harwell, in: J.F. Scamehorn (Ed.), Phenomena in Mixed Surfactant Systems, ACS, Washington, DC, 1986, ACS Symp. Ser. 311, Chapter 15.
[71] S.G. Dixit, A.K. Vanjara, J. Nagarkar, M. Nikoorajam, T. Desai, Colloids Surf. A. 205 (2002) 39.
[72] T. Gu, Y. gao, L. He, J. Chem. Soc. Faraday Trans.-1 84 (1988) 4471.
[73] S. Manne, J.P. Cleveland, H.E. Gaub, G.D. Stucky, P.K. Hasma, Langmuir 10 (1994) 4409.
[74] S. Paria, Ph.D. Thesis, I.I.T. Bombay, 2003.
[75] P.M. Holland, D.N. Rubingh, J. Phys. Chem. 87 (1983) 1984.
[76] M. Nishikido, in: K. Ogino, M. Abe (Eds.), Mixed Surfactant Systems, Marcel Dekker, New York, 1993, p. 23, Chapter-2.
[77] J.H. Clint, J. Chem. Soc. 71 (1975) 1327.
[78] P.H. Elworthy, K.J. Mysels, J. Colloid Interface Sci. 21 (1966) 331.
[79] S.H. Wu, P. Pendleton, J. Colloid Interface Sci. 243 (2001) 306.
[80] R. Atkin, V.S.J. Craig, E.J. Wanless, S. Biggs, J. Colloid Interface Sci. 266 (2003) 236.
[81] A. Sivakumar, P. Somasundaran, Langmuir 10 (1994) 131.
[82] D.M. Nevskaia, A. Guerrero-Ruíz, J. de D. López-González, J. Colloid Interface Sci. 205 (1998) 97.
[83] T. Behrends, R. Herrmenn, Phys. Chem. Earth 23 (1998) 229.
[84] P.C. Pavan, E.L. Crepaldi, G.A. Gomes, J.B. Valim, Colloids Surf. A 154 (1999) 399.
[85] J.M. Corkill, J.F. Goodman, J.R. Tate, Trans Faraday Soc. 62 (1966) 979.
[86] H. Schott, J. Colloid Interface Sci. 23 (1967) 46.
[87] B.Y. Zhu, T. Gu, Adv. Colloid Interface Sci. 37 (1991) 1.
[88] S. Partyka, M. Lindheimer, B. Faucompre, Colloids Surf. A 76 (1993) 267.
[89] F. Portet, P.L Desbène, C. Treiner, J. Colloid Interface Sci. 194 (1997) 379.
[90] P. Levitz, Langmuir 7 (1991) 1595.
[91] P. Levitz, A.E. Miri, D. Keravis, H.V. Damme, J. Colloid Interface Sci. 99 (1984) 484.
[92] P. Levitz, H.V. Damme, D. Keravis, J. Phys. Chem. 88 (1984) 2228.
[93] P. Levitz, H.V. Damme, J. Phys. Chem. 90 (1986) 1302.
[94] T.C.G. Kibbey, K.F. Hayes, J. Colloid Interface Sci. 197 (1998) 198.
[95] B.Y. Zhu, X. Zhao, T. Gu, J. Chem. Soc., Faraday Trans-1 84 (1988) 3951.
[96] D.M. Nevskaia, M.L.R. Cervantes, A.G. Ruíz, J. de D. López-González, J. Chem. Tech. Biotechnol. 63 (1995) 249.
[97] C.M.G. Gracía, M.L.G. Martín, V.G. Serrano, J.M. Bruque, L.L. Broncano, Langmuir 16 (2000) 3950.
[98] A. Tahani, H.V. Damme, C. Noik, P. Levitz, J. Colloid Interface Sci. 184 (1996) 469.
[99] N. Brack, R. Lamb, D. Pham, P. Turner, Colloids Surf. A 146 (1999) 405.
[100] J.M. Douillard, S. Pougnet, B. Faucompre, S. Partyka, J. Colloid Interface Sci. 154 (1992) 113.
[101] S.J. Clunie, B.T. Ingram, in: G.D. Parfitt, C.H. Rochester (Eds.), Adsorption from Solution at the Solid/Liquid Interface, Academic Press, New York, 1983, p. 105, Chapter-3.
[102] C.H. Giles, T.H. MacEwan, S.N. Nakhwa, D. Smith, J. Chem. Soc. Part-III (1960) 3973.
[103] R. Denoyel, J. Rouquerol, J. Colloid Interface Sci. 143 (1991) 555.
[104] S. Manne, H.E. Gaub, Science 270 (1995) 1480.
[105] S. Nishimura, P.J. Scales, S.R. Biggs, T.W. Healy, Colloids Surf. A 103 (1995) 289.
[106] W.A. Ducker, E.J. Wanless, Langmuir 12 (1996) 5915.
[107] W.A. Ducker, E.J. Wanless, Langmuir 15 (1999) 160.

[108] S. Manne, T.E. Schäffer, Q. Huo, P.K. Hansma, D.E. Morse, G.D. Stucky, I.A. Aksay, Langmuir 13 (1997) 6382.
[109] W.A. Ducker, L.M. Grant, J. Phys. Chem. 100 (1996) 11507.
[110] B.D. Fleming, E.J. Wanless, Microsc. Microanal. 6 (2000) 104.
[111] E.J. Wanless, W.A. Ducker, J. Phys. Chem. 100 (1996) 3207.
[112] E.J. Wanless, W.A. Ducker, Langmuir 13 (1997) 1463.
[113] N.B. Holland, M. Ruegsegger, R.E. Marchant, Langmuir 14 (1998) 2790.
[114] H.N. Patrick, G.G. Warr, S. Manne, I.A. Aksay, Langmuir 13 (1997) 4349.
[115] L.M. Grant, F. Tiberg, W.A. Ducker, J. Phys. Chem. B 102 (1998) 4288.
[116] J.F. Liu, G. Min, W.A. Ducker, Langmuir 17 (2001) 4895.
[117] S.B. Velegol, B.D. Fleming, S. Biggs, E.J. Wanless, R.D. Tilton, Langmuir 16 (2000) 2548.
[118] V. Subramanian, W.A. Ducker, Langmuir 16 (2000) 4447.
[119] Z. Huang, Z. Yan, T. Gu, Colloids Surf. 36 (1989) 353.
[120] J.F. Scamehorn, R.S. Schechter, W.H. Wade, J. Colloid Interface Sci. 85 (1982) 494.
[121] Y. Gao, C. Yue, S. Lu, W. Gu, T. Gu, J. Colloid Interface Sci. 100 (1984) 581.
[122] P. Somasundaran, E.D. Snell, E. Fu, Q. Xu, Colloids Surf. 63 (1992) 49.
[123] P. Somasundaran, E. Fu, Q. Xu, Langmuir 8 (1992) 1065.
[124] P. Somasundaran, L. Huang, Pol. J. Chem. 71 (1997) 568.
[125] Q. Xu, T.V. Vasudevan, P. Somasundaran, J. Colloid Interface Sci. 142 (1991) 528.
[126] K. Esumi, Y. Sakamoto, K. Meguro, J. Colloid Interface Sci. 134 (1990) 283.
[127] S. Paria, C. Manohar, K.C. Khilar, Colloids Surf. A 232 (2004) 139.
[128] J. Penfold, E.J. Staples, I. Tucker, L.J. Thompson, R.K. Thomas, Phys. B 248 (1998) 223.
[129] N.I. Ivanova, I.L. Volchkova, E.D. Shchukin, Colloids Surf. A 101 (1995) 239.
[130] T.R. Desai, S.G. Dixit, J. Colloid Interface Sci. 179 (1996) 544.